

Dispersion of solutes in porous media

A.G. Hunt^{1,a}, T.E. Skinner², R.P. Ewing³, and B. Ghanbarian-Alavijeh⁴

¹ Department of Physics and Department of Earth and Environmental Sciences, Wright State University, Dayton, OH 45435, USA

² Department of Physics, Wright State University, Dayton, OH 45435, USA

³ Department of Agronomy, Iowa State University, Ames, Iowa 50011, USA

⁴ Department of Earth and Environmental Sciences, Wright State University, Dayton, OH 45435, USA

Received 20 October 2010 / Received in final form 5 January 2011

Published online 24 March 2011 – © EDP Sciences, Società Italiana di Fisica, Springer-Verlag 2011

Abstract. A recently introduced theory of solute transport in porous media is tested by comparison with experiment. The solute transport is predicted using an adaptation of the cluster statistics of percolation theory to critical path analysis together with knowledge of how the structure of such percolation clusters affects the time of transport across them. Only the effects of a single scale of medium heterogeneity are incorporated, and a minimal amount of information regarding the structure of the medium is required. This framework is used to find effectively the distributions of solute velocities and travel distances and thus generate arrival time distributions. The comparison with experiment focuses on the dispersivity (the ratio of the second to the first moment of the spatial solute distribution). The predictions of the theory in the absence of diffusion are verified by comparing with over 2200 experiments over length scales from a few microns to 100 km. At larger length scales (centimeters on up) about 95% of the data lie within our predicted bounds. At smaller length scales approximately 99.8% of the data lie where we predict. These comparisons are not trivial as the typical values of the dispersivity increase by ten orders of magnitude over ten orders of magnitude of length scale. Noteworthy is that the classical advection-dispersion (ADE) equation predicts that the dispersivity should be independent of length scale! This agreement with experiment requires rethinking of the relevance of diffusion and multi-scale heterogeneity and would also appear to signal the complete inappropriateness of using the classical ADE or any of its derivatives to model solute transport.

1 Introduction

Dispersion of solutes in fluid flow occurs under the influences of spatially varying velocities and microscopic diffusion. Although natural conditions “in the field” also normally involve temporally dependent velocities, functions that describe solute behavior are typically defined under steady-state conditions. The various constituents of geological porous media (solid, air, water, oil, etc.) are distinct. At the scale of individual pores, solutions of differential equations for fluid flow, electrical conduction, and solute transport require specification of boundary conditions along the surfaces bounding these constituents. In the case that a response function, such as to a pressure gradient, will be either zero (in the solid) or finite (in a fluid), the result is that the fluid flow must be zero at the interface. Using a continuum approach to predict system-wide response by solving the same differential equations at large length scales for which such a pore-solid boundary condition cannot be specified could lead to problems. Consequently, using the advection-dispersion equation (ADE) from continuum mechanics as a starting point for describ-

ing solute dispersion in porous media (e.g., Ref. [1]) is questionable, particularly as its predictions for the spatio-temporal evolution of solute plumes are rarely correct. Moreover, questions regarding the applicability of this equation to dispersion in porous media have been raised previously (e.g., Refs. [2–4]).

In this work we consider a completely microscopic derivation of the relevant transport parameters, developing a general theory of solute dispersion in porous media. But before we introduce our approach, we first discuss what it is that the ADE does not accomplish. In so doing we present the problem that others have tried to solve, and provide a basis for understanding what is unique about our solution.

2 Relevance of problem

The question of how best to describe solute transport in porous media, especially at geological spatial scales, can generate interest from many quarters. Of course users, such as monitors, stewards, and regulators of toxic solutes, need to be able to predict their spreading as fluids

^a e-mail: allen.hunt@wright.edu

migrate through the subsurface. Theoreticians are interested in the fundamental mismatch between existing theory and observation. Experimentalists wish to optimize their experimental design and undertake investigations that discriminate between theories. It may be that our discussion is relevant to many other current subjects of research as well [5]: “the migration apart of initially adjacent molecules under flow and diffusion underpins processes as diverse as cellular mitosis, blood perfusion in the brain, chromatography, filtration, secondary oil recovery, ground water remediation, catalysis, and the behavior of packed bed reactors”. Other applications of the ADE include as wide a range of topics as degradation of building materials [6,7], tissue physiology [8], migration and epidemiology [9,10], as well as heat dispersion in foams [11] and even the internal dynamics of the atom [12]. In this review we will not attempt to determine how well the physics or predictions of the ADE are matched to these other problems. That is, the questions of how well the existing theory of transport in groundwater represents the physics of other systems, or of how closely related solute transport in porous media is to other specific systems, are not addressed here. We will only investigate the case of solute transport through porous media, concentrating our attention on geological cases.

3 Extant theory

3.1 The advection-dispersion equation (ADE)

Consider a piecewise homogeneous medium. The ADE generates the temporal change of solute concentration at a given point (within the boundaries) by considering advection and diffusion processes independently. Here advection means that flow at the smallest spatial scale brings to any given location a solute concentration that existed just upstream, and is expressed as the (negative of the) inner product of the local fluid velocity, \mathbf{v} , with the solute concentration gradient, ∇C . The diffusion term, in accord with linear response theory, relates the temporal change in concentration at a point, $\partial C/\partial t$ to the Laplacian of the solute concentration at that point. Thus the entire equation is,

$$\frac{\partial C}{\partial t} = D_h \nabla^2 C - \mathbf{v} \cdot \nabla C. \quad (1)$$

The diffusion term results from combining the effects of transport linear in the concentration gradient with the equation of continuity, but the analog to the diffusion constant, called the “hydrodynamic dispersion”, D_h , is not clearly defined as we will see. The ADE is more or less universally accepted to be correct at the scale of one pore [13]. But its predictions are not borne out at any scale larger than this [14–22]. Writing the Laplacian as the divergence of the product of a (spatially-dependent) transport coefficient and the concentration gradient, introducing an additional term (the scalar product of the gradients of the transport coefficient and the concentration), only addresses spatial variability in the continuum

description of the medium, not the possibility that the continuum description is inappropriate.

3.2 Limitations of the ADE

The failure of the ADE is probably more a question of its inadequacy in treating the discrete differences in the medium than in its treatment of the heterogeneity that represents variations in the pore space. However, its inadequacy in treating local variations in pore velocity have also been shown to have serious consequences ((2) next paragraph) [23,24]. Further, the ADE also does not work at spatial scales large enough [2,3] that the dominant heterogeneity is described in geologic terms, for which discretization of the medium may be preferred [4], but is not a requirement.

The most prominent failures of the ADE are: (1) its inability to predict the late-time enhancement of solute arrivals [4,15–17] (which more resemble a power-law than a Gaussian form), (2) the need to introduce scale-dependent coefficients [14,18,19], such as the hydrodynamic dispersion (the generalized diffusion coefficient), D_h , coupled with the inability to predict these scale dependences, and (3) the inability to predict the enhancement of solute arrivals at early times [16]. The failures in (1) and (3) have been known for over 50 years [25]. The failure in (2) is quite spectacular; the ADE in a homogeneous medium predicts a scale-independent ratio of the second and first moments of the solute distribution (called the dispersivity), where in fact the dispersivity increases by 10 orders of magnitude over ten orders of magnitude of spatial scale [19,20,22].

Because the observed solute spreading clearly exceeds that attributable to molecular motions, the Laplacian term in the ADE has been re-defined as “hydrodynamic dispersion”, while it was still considered mathematically consistent with diffusion. Diffusive transport requires long-time behavior consistent with the central limit theorem (CLT); the variance of the solute plume must increase linearly with distance and time. However, solute arrival time distributions generally have “fat” (power-law) tails [15–17] and variances that increase superlinearly [18–20] over many orders of magnitude of length and time scales. In most cases, and at scales larger than a single pore, the high predictability of experimental results for the dispersivity using our theoretical approach under conditions that diffusion can be ignored indicates that advection is the only relevant mechanism for dispersion, so it is better to drop the diffusion term altogether. But the simple concept of advection of a solute front is completely inadequate to describe the process of solute dispersion, so the second term in the ADE does not suffice on its own, and the entire equation is best abandoned at scales greater than a single pore. We argue that use of the ADE has led to great confusion in understanding what physical processes are relevant to dispersion. In our theoretical approach only about 3% of well over 2000 experimental results fall outside our range of prediction, even though we neglect diffusive processes altogether!

This review will describe how these conclusions become inescapable in groundwater transport.

3.3 Modifications of the ADE

Probably the most widely used alternative to a simple application of equation (1), called stochastic subsurface hydrology, is based on a perturbative solution of stochastic differential equations. Equation (1) becomes stochastic when the coefficients have a random spatial variability. While a significant length dependence of the dispersivity can be generated using this theory [13] it cannot account for such variability, noted above, over ten orders of magnitude of spatial scales.

The continuous time random walk (CTRW) has also been applied [14–17] to solute transport in porous media, but its relationship with the present formulation is rather complex and we will defer discussion of this point until later. We suggest that the CTRW, when properly informed by the percolation framework given here, may in fact be the best approach to solute transport. But the CTRW does not supply the parameters and functions needed as input nor does it, by itself, give a means to determine these from medium characteristics.

Another means employed to overcome defects of the ADE is to change the order of the differentiation in this equation to fractional (FADE) [24,26–32]. This change in the order of the differentiation is consistent with assuming that particles follow Levy flights rather than Brownian motion [26–29]. The references in [28,29] both address Levy Flights on finite-size domains, but with reflecting boundaries and absorbing boundaries, respectively. Such fractional differentiation can also be combined with spatially variable parameters, effectively generating stochastic fractional order differential equations. The FADE can build in the observed long-time behavior (“fat tails”) of solute transport, but it lacks the theoretical basis of the ADE at the scale of a single pore. In effect it is consistent with choosing an altogether different fundamental mechanism for solute transport. Since such a treatment generates interpretations akin to those for emergent phenomena, it does not foster investigation of relationships between equation parameters and media characteristics; in particular, no clear method has been found to relate the (fractional) order of the derivative to any property of the medium. Further, fractional differential equations do not generate the enhanced solute arrival at short times [16]. Finally [33] even use of the FADE may not avoid unpredictable scale dependences in its coefficients. Nevertheless, when we discuss the relationship of percolation and the CTRW, a certain resemblance of the particle motions we derive (incorporating diffusion) to Levy flights will be seen.

4 New theory

4.1 Motivation

One of the most oft-cited inadequacies of traditional solutions of the ADE is their insensitivity to connectivity, in

particular the relevance of well-connected areas of more highly conductive regions [34–38]. Connectivity, even in geologic systems, is really the subject of percolation theory [39,40] and this particular review will describe how the understanding of solute transport in porous media is changed by adopting a theory of connectivity in the context of heterogeneous transport. This particular theoretical approach has already been developed and published in several articles [41–44] as well as a book [40], but its predictions have only recently been subjected to more thorough comparison with experiment [43,44] (also here), and it is chiefly the superiority of its ability to predict solute dispersion that makes this percolation treatment of solute transport of particular interest.

In contrast to stochastic subsurface hydrology, percolation theory, in an application incorporating only effects of advection, generates the exact result for the dispersivity in a medium with only a single scale of disorder, and produces the correct forms of solute arrival enhancement at short and at long times as well [42–44]. We should mention that, while our percolation treatment reproduces the scale-dependence of the dispersivity, it only generates the experimentally observed distribution of dispersivity values when applied separately at two different scales of heterogeneity, one for micromodels and the second for (so far) all other experiments; this issue will be discussed in more depth below.

The major research thrusts of several of the U.S. National Science Foundation programs and cross-directorate competitions are to address the scale dependences of such coefficients for heterogeneous media or for non-linear governing dynamic equations (such as Navier-Stokes) or both. Since stochastic subsurface hydrology [45–47] can only generate a significant scale-dependence using multi-scale heterogeneity [13], the notion has arisen that only projects that address multiple scales of heterogeneity are worthy. Such multi-scale heterogeneity is treated typically in one of two contexts: either advanced numerical techniques [48–52] (applied mathematics and civil engineering), or stochastic [53] of the associated Sturm-Liouville equations [54,55]. But perturbation theory cannot be used unless the disorder in the medium may, in some sense, be classed as small; otherwise the series does not converge. Further, for calculating effective properties of disordered semi-conductors and related systems, perturbation theory was supplanted by percolation or effective-medium theories long ago [56]. We also do not advocate approaches based on advanced numerical techniques, since they seldom provide grounds to develop physical understanding, while those based on the ADE (the majority) may not contain the appropriate physical basis anyway. Another drawback of numerical methods is the huge amount of information required to model the medium accurately (particularly when multiple scales of heterogeneity are addressed) coupled with insufficient understanding regarding which characteristics are actually relevant.

Our framework was not developed to address any of the particular problems discussed in the introduction. Rather, it developed as a logical outgrowth of work included in the

1st edition of “Percolation theory for flow in porous media”. [57] After the research paper on solute dispersion was published [42], its basic derivations could be incorporated into the 2nd edition of “Percolation theory for flow in porous media” [40] since like other medium properties it was calculated combining concepts from critical path analysis, percolation cluster statistics, and percolation scaling. However, the large improvement in predictability resulting from use of percolation theory leads us to a fundamental discussion regarding the physical basis of the dispersion. That is, our discussion has implications (repercussions) well beyond the present context.

4.2 Fundamental concepts and critical conductance

Our approach is a blending of concepts from random resistor networks [58] and percolation theory [59]. Thus we use first whatever microscopic theoretical approach is appropriate to calculate values of resistances between nodes in a network. In solid state systems this could be Fermi’s golden rule from quantum theory, while in porous media we simply apply properties of viscous flow. Then we use percolation scaling [60], cluster statistics of percolation theory [61] and concepts from critical path analysis (CPA) [62,63] – itself an application of percolation theory – to find the macroscopic transport properties. While we cannot guarantee that our approach is valid in all the systems listed in the introduction, it is likely to be useful for calculations of dispersive transport in disordered semiconductors. The continuous time random walk [64,65], utilized in a number of recent publications on groundwater transport [15–17,66], had originally been used in this context (e.g., [67]).

Percolation theory can be formulated in terms of sites, bonds, or the continuum. We introduce our framework for calculation in terms of bond percolation because each bond can correspond to a conductance, g . We first define the bond probability and its critical value from percolation theory. The probability of connecting an arbitrary bond in a bond percolation problem [59] is taken as p . The smallest value of this probability for which percolation occurs is defined [59] as p_c . To find the critical conductance [62,63] all we need from percolation theory is the value of p_c . p_c is strongly system dependent, making its value difficult to predict in natural systems. The difficulty in predicting p_c makes CPA a somewhat unpopular subject of percolation theorists. But a logical approach based on percolation theory, if it is to be valid for any medium, whether near or far from the percolation threshold, must start from a basis which allows incorporation of the effects of a distribution of conductance values.

CPA uses the critical percolation probability, p_c , from percolation theory to isolate and define that portion of a network that makes the dominant contribution to conduction (or flow). Consider the process of removing all the resistances from a random resistor network and then replacing them in order of increasing resistance. With increasing resistance value the number of connections in the

network increases and after a while clusters of interconnected resistances appear. At the percolation threshold at a critical resistance (or conductance) an infinite cluster of interconnected resistances form which would connect opposite sides of an infinite system. The last resistance emplaced is the largest resistance (or smallest conductance) that an interconnected current path cannot avoid. Put another way, this last resistance is the smallest possible value of the largest resistance on a path connecting opposite sides of an infinite system. In everyday language we could call this a bottleneck resistance. The system conductivity is then closely related to the critical resistance. Knowledge of the value of p_c will turn out to be of secondary importance; its greatest effect is in fixing the time of the peak solute flux, which is not our focus here. Nevertheless, we will generally use percolation theoretical techniques to relate local to global quantities, making percolation our strategy for “upscaling”. Note that the search for such upscaling has been a goal of the porous media communities for decades, but only Sahimi [68,69] has been consistently cognizant of the relevance of percolation theory over this period.

The theory outlined here combines two aspects of percolation theory. Firstly, we use cluster statistics of percolation theory to find the probability that a given system is traversed by a cluster of interconnected conductances with arbitrary minimum value. Secondly, we apply knowledge of the topology of such clusters to find the time required for solute to traverse them. These can both be expressed in terms of the critical conductance. In the language of CPA the second point can be used to describe the lengths and velocities of solute paths, the frequency of occurrence of which is then defined by the first point. This means of calculation accounts only for dispersion due to different velocities and entirely neglects diffusion. It is thus strictly valid only for infinite Peclet number (ratio of diffusion to advection times) [70], which one might not expect to be useful in practice. However, the vast majority of experiments appear to be consistent with this result. Later we show how to account for diffusion effects in lowest order for large Peclet number [43] and when we compare with experiment we find that our predictions work for Peclet number as low as 1.

While CPA has traditionally been developed in terms of an infinite network, it can also be approached from the cluster statistics [61] via the first aspect of percolation mentioned above. Note that that calculation also yields the probability that a particular system is spanned by a cluster with minimum conductance equal to the critical value, g_c . In the limit of infinite size the cluster statistics vanish for values of g other than g_c . This restriction has profound effects on the moments of the solute distribution for large system size.

With the conceptual approach outlined above, we now consider more concretely how flow (or conduction) can be represented in terms of a random resistor network. Nodes represent places where flow paths can join or diverge from, and the ease of flow in the links between the nodes is described by a distribution (in the sense of a probability

density function), $W(g)$, of conductances, g . If water flow at the pore scale is considered, then the nodes and links could correspond to pores and pore throats, respectively. Representing pore throats by an equivalent right circular cylinder relates the local flow rate, q to the local pressure drop ΔP by,

$$q \propto \frac{r^4}{l\mu} \Delta P \propto g \Delta P. \quad (2)$$

The local conductance, g , is therefore proportional to the fourth power of the radius, r , of the pore throat, and inversely proportional to the viscosity, μ , and the pore throat length, l . On either a regular network, for which l is a constant, or on a fractal structure (with $l \approx r$), the conductance distribution, $W(g)$, would then derive from the pore radius distribution.

CPA determines the critical conductance, g_c , of $W(g)$ by taking an integral over all conductances greater than or equal to g_c and setting it equal to the critical bond fraction, p_c ,

$$\int_{g_c}^{\infty} W(g) dg = p_c. \quad (3)$$

The value g_c is then the largest possible value of the smallest (bottleneck) conductance on a path of interconnected conductances guaranteed to span an infinite system. For porous media g_c also describes the conductance of the smallest pore radius on the optimal path through the system. Clearly such a critical conductance value is of relevance for determining effective conductivity, and for systems with wide ranges of local conductivity values it is usually considered the best way to do so [71–73]. This concept from CPA is also what is used to organize the calculations of solute dispersion and might be assumed to restrict the relevance of these calculations to very strongly disordered systems. In fact it seems appropriate for all magnitudes of flow disorder.

4.3 Solute distributions

Calculations of the temporal and spatial solute distributions are described here in outline form since they are given also in references [40–42]. However, we have made some minor changes in notation since reference [42]. Suppose water flows steadily through some porous medium of arbitrary length. At some initial instant a pulse of solute is introduced uniformly over the dimensions of the system transverse to flow, i.e., $C(0, t) = C_0 \delta(t)$. We want to know the distribution of solute arrival times at some distance downstream, expressed in e.g. soil physics and environmental engineering as a breakthrough curve.

We define $W_p(t; x) dt$ as the probability, obtained from percolation arguments, that a solute particle introduced at time $t = 0$ will arrive at a downstream distance x a time within dt of t . Since each particle must arrive at x at some value of t (if adsorption processes are neglected), $W_p(t; x)$ is normalizable over the variable t and $W_p(t; x)$ becomes the arrival time distribution for flow over a distance, x . Multiplication of $W_p(t; x)$ by C_0 yields the predicted time

dependence of the solute concentration along the transverse plane at distance x . If a time dependent concentration is introduced, Green function techniques can easily develop the downstream concentration. In the case that $C(0, t)$ is a step function (a common experimental technique) rather than an instantaneous pulse, the downstream concentration $C(t, x)$ is the integral of $W_p(t'; x)$ over the interval $0 < t' < t$. Note that in the case of a Gaussian distribution, a breakthrough curve (as an integral over a Gaussian) would translate to the error function, which approximately accords with many plots of experimental data.

We define $W_p(x; t) dx$ as the probability, obtained from percolation arguments, that after time t has elapsed, such a solute particle has traveled a distance within dx of x downstream from its point of introduction. Both $W_p(t; x)$ and $W_p(x; t)$ are obtained from the cluster statistics of percolation theory. Once $W_p(x; t)$ is known, the dispersion coefficient, $D_l(t)$, and the dispersivity, $\alpha(x)$ can both be determined from its second moment (variance) [74]. This calculation is possible even when the variance of the arrival time distribution is undefined (on account of its long-time tail), since the long tail in the spatial distribution is cut off by the point of introduction of the solute (absent diffusion).

Although we defined our terms in the language of bond percolation, all the results can and will be equivalently represented using continuum percolation. The definition of bonds and nodes in the second paragraph of 4.2 shows how the bond and continuum percolation formulations can be easily related for porous media. The dependence of the arrival time of individual particles that traverse such a cluster on the Euclidean size of the cluster derives from the mass fractal dimensionality of the backbone.

4.3.1 Steps in the calculation

(A) The volume concentration of clusters having s interconnected bonds is a function of both the difference $p - p_c$ and the number of bonds, s . Adapt the cluster statistics of percolation theory, given in terms of s and of $p - p_c$, to the linear extent of the medium and to specific values of the smallest conductance on such a cluster, g , as well as its critical value, g_c . This is accomplished by equating the cumulative distribution from $g(g_c)$ to infinity with probability $p(p_c)$. Since we have argued [40, 75] that fractal models should be treated in continuum percolation theory, in practice we use the volume fraction V and its critical value, V_c , in place of p and p_c .

(B) Integrate the cluster statistics over all clusters larger than or equal to the system size to find the probability density function, $W_p(g; x)$. This gives the probability that a system of length x can be spanned by an interconnected cluster of conductances with minimum conductance, g .

(C) Use what is known about the tortuosity of such clusters to find the time, $t(g)$, required for solute to traverse them.

(D) Calculate $W_p(t; x) = gW_p(g; x)/(dt(g)/dg)$. The reason for the extra factor g is that, for uniform concentration of introduced solute, the solute flux must be proportional to the water flux, and the probability that a solute particle arrives at a given distance differs from the probability that such a cluster actually exists.

4.3.2 Calculation of the dispersion coefficient for a specific model

(1) Describe the medium. We chose the Rieu and Sposito [76] discrete random fractal model adapted for a continuous distribution of pore sizes [75]. The same model can be applied at the pore scale [75] or at geologic scales [77], where the analogy to the pore and solid portions of the medium are high and low permeability regions, respectively. This makes the volume fraction of the more permeable portion the analogue to the porosity.

For a fractal medium, pore lengths should, on the average, be proportional to pore radii ($l \propto r$). The probability density function (pdf) representing the fraction of pore volume in pores of radius r is $W(r) = (3 - D)r^{2-D}/r_m^{3-D}$. Here D is the fractal dimensionality of the pore space and r_m is the radius of the largest pore. Integrating the pdf from the smallest pore, r_0 , to r_m yields a known result [76] for the porosity, $\phi = 1 - (r_0/r_m)^{3-D}$. When inertial effects in the flow are not important, i.e., for low Reynolds number flow, Poiseuille's law for flow in a right circular cylinder (Eq. (2)) can be generalized to yield an expression for the pore conductance, which then allows development of a pdf for pore conductances. Since the total mass flux would be proportional to the fourth power of the radius of the cylinder and inversely proportional to its length, the hydraulic conductance of the cylinder is proportional to the cube of the radius. The hydraulic conductivity of the cylinder, however, is proportional to the square of the radius. Then a medium composed only of pores of radius r_0 (r_m) would, by Miller-Miller similitude [78] have a saturated hydraulic conductivity, $K_0(K_m)$ proportional to $r_0^2(r_m^2)$. Thus the ratio r_0/r_m is proportional to $(K_0/K_m)^{1/2}$. This representation in terms of conductivities is required for larger scale applications, since, e.g., sandy and silty portions of a medium of lengths decimeters to tens of meters, for example, may have large contrasts in hydraulic conductivities, but do not correspond directly to pores of meter size.

Direct application of [76] to larger length scales is thus possible when the medium is composed, e.g., of two different sediments and when each is heterogeneous [77]. Then, if the more permeable portion of the medium comprises 25% of the sediment and it is, on average, 10 000 times as conductive as the less permeable portion, $3 - D = \log(1 - 0.25)/\log(1/10\,000^{1/2}) = 0.06$ and the fractal dimensionality of the Rieu and Sposito [76] analogue would be 2.94.

(2) Apply A above. In order to generate predictions with a minimum number of adjustable parameters, it is useful to have a specific value for the critical volume fraction, V_c , for percolation. V_c is known empirically [79] as

the moisture content at which the diffusion constant vanishes; following [79] we call this moisture content θ_t . This inference is sensible since one would expect solute diffusion to vanish [80] when the water content of the medium is so low that the water is not continuous. The pdf for the pore space, $W(r)$, must next be transformed to a pdf for the conductance, $W(g)$ by using the appropriate dependence $r = r(g)$. At the pore scale [42], the proportionality $g \propto r^4/l$ with pore length $l \propto r$ leads to $g \propto r^3$, or $r \propto g^{1/3}$. Finally, normalize $W(g)$ so that an integral of $W(g)$ over all g gives one. Then an integral over $W(g)$ from g_c to $g_m \propto r_m^3$ yields V_c , defining g_c . At larger scales [77] the procedure is completely analogous, but V_c is not typically known.

(3) Calculate, using procedure B above, the probability, $W_p(g; x)$ that a finite cluster of conductances g can be constructed to span a system of length x . Since an arbitrary volume fraction may be related to g in the same way as V_c relates to g_c , the variables $V - V_c$ can be transformed [42] to $g^{1-D/3} - g_c^{1-D/3}$. Scaling laws of percolation allow relation of s to the linear dimension, x , of a cluster [75,81]. Finally, any cluster with Euclidean length greater than or equal to x can connect opposite sides of a system of size x , so that an integral over cluster sizes larger than x must be performed in order to generate the desired probability. The result for $W_p(g; x)$ is given in terms of the exponential integral [42],

$$Ei[z] = \int_z^\infty \exp[-y]dy \quad (4)$$

as,

$$W(g; x) \propto \frac{1}{b} Ei \left[a \left(\frac{x}{L} \right)^b \right] \quad (5)$$

with L the correlation length (the cube of which is known as the representative elementary volume, REV [75,82]) and the parameters a and b are defined below,

$$a = \left| 1 - \left(\frac{g}{g_c} \right)^{\frac{3-D}{3}} \right|^2 \quad \text{and} \quad b = \frac{2}{\nu}. \quad (6)$$

Here ν is the exponent that describes the divergence of the correlation length at the percolation threshold.

The calculation of L in [82] is a straightforward application of percolation theory, in which the correlation length is given as the product of a fundamental length scale and the percolation theoretical expression. In CPA at the pore scale, however, this calculation [75] involves an optimization between geometry (defined through the critical conductance) and topology (the constraint that a system conductivity defined through the infinite cluster right at percolation is zero). It was concluded [75] that L on a lattice was a characteristic length scale in the "optimal" network, which carried the dominant steady-state flow. In practice [75] a good order of magnitude estimate of L at the pore scale was 10 times the typical lattice separation, which translates here to 10 times a typical pore separation. At larger scales [77] the inference is that L

would be about 10 times the length of a typical geological unit.

(4) Calculate the expected time, $t(g)$, of transit for particles on such a cluster (point C above), i.e., how long it would take a particle on the average to reach the right side if it entered the left side at an arbitrary position at an initial time (C above). The result is [42],

$$t(g) = \left(\frac{x}{L}\right)^{D_b} \frac{t_0}{3-D} \frac{1}{(1-\theta_t)^{\nu D_b - \nu}}$$

$$\times \left[\left(1 + \frac{\theta_t}{1-\theta_t}\right) \left(\frac{g_c}{g}\right)^{1-D/3} - 1 \right]^{(D_b-1)\nu}$$

$$\equiv \left(\frac{x}{L}\right)^{D_b} t_g. \quad (7)$$

Here t_0 is a typical time for solute transport across a single pore, which is dependent on the fluid velocity and thus the pressure difference and the conductance of the pore. D_b is the mass fractal dimensionality of the backbone cluster. θ_t is the critical moisture content for percolation or equivalently the critical volume fraction for percolation, and x is the system length. While equation (7) turns out to be valid for both saturated and unsaturated systems [42], we have not examined the limits on its validity in detail and presume that it is only valid to a minimum saturation well above the critical value.

Result (7) for $t(g)$ has two basic inputs. One is from the pore size distribution (a sum over resistances less than $R_c = 1/g_c$, with additional justification below) and generates a non-critical dependence on g/g_c . The second input derives from the tortuosity of the paths on the cluster and generates a critical dependence on g/g_c (i.e. a divergence) with power $(D_b - 1)\nu$. The tortuosity is calculated according to the Mandelbrot [83] definition of a fractal dimension, but with a somewhat non-intuitive substitution. One might naively expect the relevant exponent to be that describing the transit distance (the optimal path exponent [84]), but reference [85] demonstrates that the transit time follows a different divergence given by the mass fractal dimensionality of the backbone, D_b . Values of D_b for various percolation models are tabulated in reference [60]. The implications of choosing only a single cluster-crossing time rather than a distribution of such times [85] are discussed later.

In the calculation of $t(g)$ above, the effects of the pore-size distribution are complicated, but calculations can be simplified by assuming that the path is one-dimensional [86,87], conserving the flux on that path. Then the time is just the sum of the times spent individually in each conductance (an analogy to the total resistance, which is a sum of the resistances) where the occurrence of a conductance with value $g > g_c$ is assumed governed by the same statistics as in the bulk of the medium. This last assumption is imperfect [88], but it is typically used [86,87] anyway, because the actual distribution, while similar, is not known precisely [88]). As long

as the entire distribution of conductances greater than the critical value is sampled over a distance less than the typical separation of branches of the path, this calculation of the first factor does not contradict the calculation of the second, which arises from the tortuosity and complex interconnectedness of the paths.

(5) Apply point D above.

(6) Calculate the spatial distribution, $W_p(x;t)$ at an instant in time by an analogous procedure, noting that x is now proportional to t^{1/D_b} and normalize [42].

(7) Calculate the variance of the spatial distribution from $W_p(x;t)$ as $\langle x^2 \rangle - \langle x \rangle^2$, where $\langle x^2 \rangle$ is the second moment of the distribution and $\langle x \rangle$ is its mean. The integration over x makes the variance explicitly a function of time only. However, since the typical time of transport relates deterministically to the transport distance (via Eq. (7)), the variance may be represented as a function of typical travel distance.

(8) The deviation from Gaussian behavior in time is typically represented by use of the longitudinal dispersion coefficient [67], $D_l(t) \equiv \frac{1}{2}d/dt[\langle x^2 \rangle - \langle x \rangle^2] \approx [\langle x^2 \rangle - \langle x \rangle^2]/t$. The factor 1/2 arises because the variance is the square of the width, σ , of a Gaussian distribution. Notice that for Gaussian dispersion (variance linear in t), $D_l(t)$ would be a constant, since in that case $\sigma = (D_h t)^{1/2}$ and $D_l(t)/t = D_h t/t = D_h$. Thus the experimentally determined longitudinal dispersion coefficient has been used to guide the application of the ADE at larger scales through the choice of the same scale dependence for the hydrodynamic dispersion. The dispersion coefficient may also be represented as a function of the typical travel distance, just as the variance.

(9) The deviation from Gaussian behavior in space is typically represented in terms of the dispersivity $\alpha \equiv [\langle x^2 \rangle - \langle x \rangle^2]/\langle x \rangle$. If, as expected from equation (1), Gaussian behavior with a time-independent velocity, v , were actually observed, the dispersion coefficient and the dispersivity would be essentially equivalent measures, with $D_l(t) = D_h$, from equations (1) and $\alpha = tD_h/vt = D_h/v$. Writing the dispersivity as the ratio of the dispersion coefficient and the average velocity is quite generally valid, as long as the velocity is allowed to be a function of spreading distance. In this formulation dispersivity α is generated directly as a function of t , but it can also be plotted as a function of $\langle x \rangle$, since both are monotonically increasing functions of t .

(10) Choose parameters. We chose the fractal dimensionality, D from the random fractal model that would make the medium either highly ordered (a very small ratio, e.g., 1.1 of largest to smallest conductance) or quite disordered (a ratio that could be as large as 100 000). These choices corresponded to $D = -1$ and $D = 2.97$. We chose a critical volume fraction (15%) for percolation nearly equal to the value known [89] since 1970 to provide a good general estimate in porous media. The exponents from percolation theory, such as the exponent for the correlation length and the fractal dimensionality of the backbone, are specified in references [59,60]. Note that the correlation length exponent is universal and takes on

the values 0.88 in 3-D and $4/3$ in 2-D. The fractal dimensionality of the backbone, however, depends on the percolation system considered [60] with values for invasion percolation [90] that can be smaller than in random percolation. Invasion percolation, in which the defending fluid can remain trapped in pockets (like air bubbles), is called in reference [60] “invasion percolation with trapping”, and is relevant whenever the defending fluid is incompressible (always in our case). Such invasion percolation models are thought to be relevant in fracture flow when air is trapped, and may be relevant in soils at smaller scales as well. In our particular calculations the relevance is that the invasion percolation backbone tends to be less tortuous, producing a smaller dispersivity, but a larger dispersion coefficient (since with a minimally tortuous path the velocity barely diminishes with distance).

5 Results and discussion

We choose to present the results and discussion for the theoretical development in the absence of diffusion before we introduce the expected effects of diffusion. This helps define the relevance of the diffusion process to lab and field scale experiments as well as to provide some guidance as to how to incorporate diffusion effects into the theory.

5.1 Construction of the arrival time and spatial distributions

We present first the results for both $W_p(g; x)$ (Fig. 1) and $t(g)$ (Fig. 2). Although these quantities cannot be compared directly with experiment at this time, we think it is very instructive to show them since, individually, they bear no resemblance to the experimental results for $W_p(t; x)$; it is only when $W_p(t; x)$ is constructed via procedure D above that a recognizable result emerges (Fig. 3). Note that neither $W_p(g; x)$ nor $t(g)$ is particularly sensitive to the parameters, D and V_c , although we do not show this here (see Ref. [42]). In order to apply the identity in procedure D we must be able to identify all the limiting conductance values, g (smallest conductance on the path), for which the transit time is the same. For small system sizes there are frequently three such g values. Even though equation (7) is relatively straightforward, its combination of (potentially) irrational powers makes its inversion a strictly numerical problem involving a rather difficult interpolation near the peak.

In Figures 3 and 4 we show characteristic results for $W_p(t; x)$ and $W_p(x; t)$. These also are not very sensitive to variations in the parameters D and V_c , although the long time (for $W_p(t; x)$) and short travel distance (for $W_p(x; t)$) tails do depend sensitively on whether flow is two or three dimensional and on whether the appropriate model is invasion or random percolation. Note that the region near the peak of the distribution is influenced through CPA more strongly by the statistics of the conductance distribution, whereas the long tails in $W_p(x; t)$ and $W_p(t; x)$ arise from particles following paths near the percolation

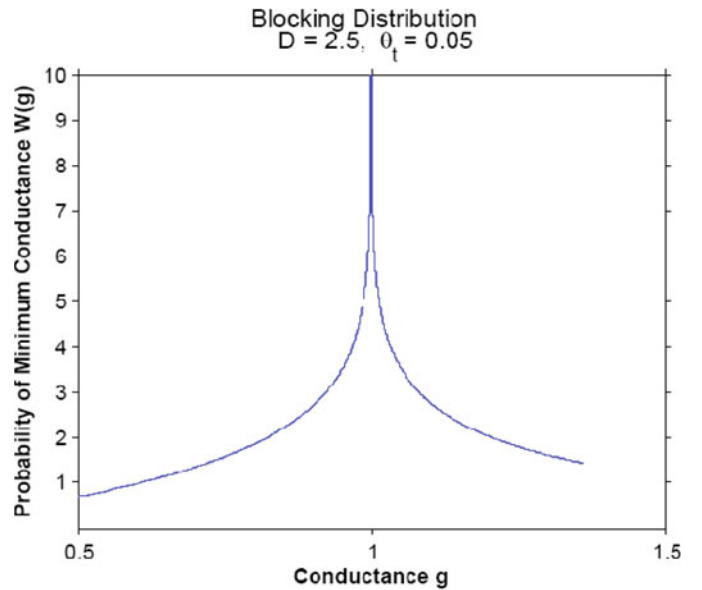


Fig. 1. The probability density function, $W_p(g; x)$, for the minimum conductance value, g , on a cluster that spans a system of linear dimension x . Note the logarithmic divergence at the critical conductance, g_c , which was defined as 1. The logarithmic form is the leading term in an asymptotic expansion of the exponential integral, equation (5). This figure, from [42], was drawn using an older notation; the designation “blocking distribution” refers to the fact that g is a blocking, or minimum, conductance. The value of the fractal dimensionality for the Rieu and Sposito model [76] and the critical moisture content, θ_t , are given.

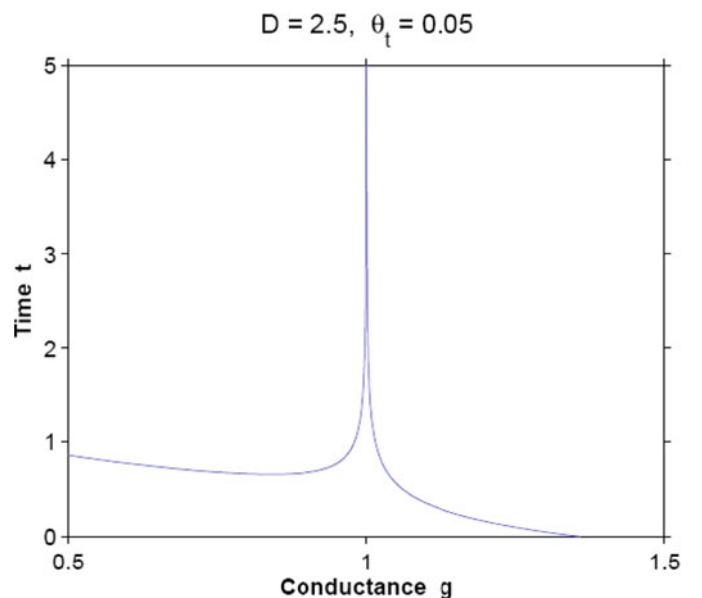


Fig. 2. The conductance, g , dependence of the time, t , of transit for solutes that cross a cluster with minimum conductance g . The parameter values are given again. Here the critical conductance g_c is again defined as 1. In this case the divergence has a power-law dependence. Figure is again from [42].

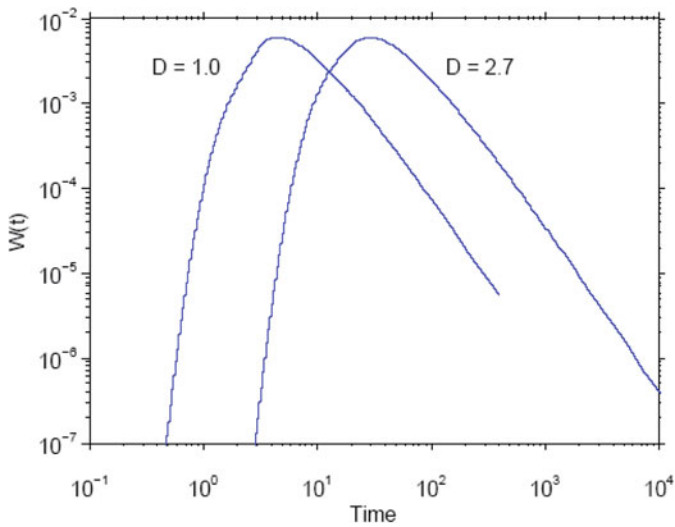


Fig. 3. The time t dependence of the arrival time distribution for an arbitrary plane downstream of the introduction of the solute, denoted on the y -axis as $W(t)$, and the relative insensitivity of its shape to the fractal dimensionality of the pore space. Axes are logarithmic scales. Figure is also from [42].

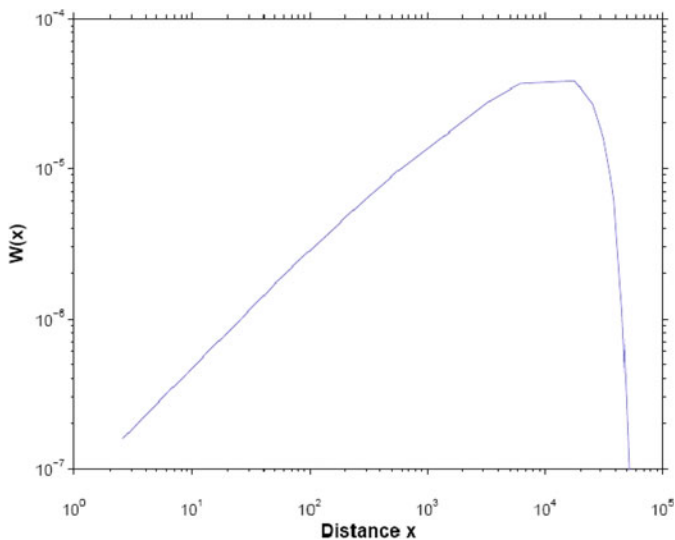


Fig. 4. The spatial dependence, denoted on the axis as $W(x)$, of the solute distribution at arbitrary time x and for representative values of the critical volume fraction for percolation and fractal dimensionality D . Axes are logarithmic scales. Figure is from [43].

threshold with very large tortuosity. If particles diffuse off such paths, then the long tails in the distributions should disappear [43]. This gives a motivation for estimating the effects of diffusion in terms of a probability that a particle will remain along such a path.

5.2 Features of the distributions

The arrival time distribution in two dimensional systems governed by random percolation has an approximately

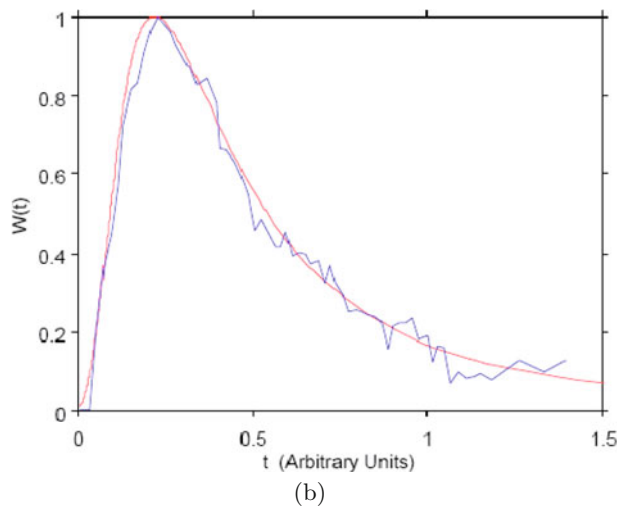
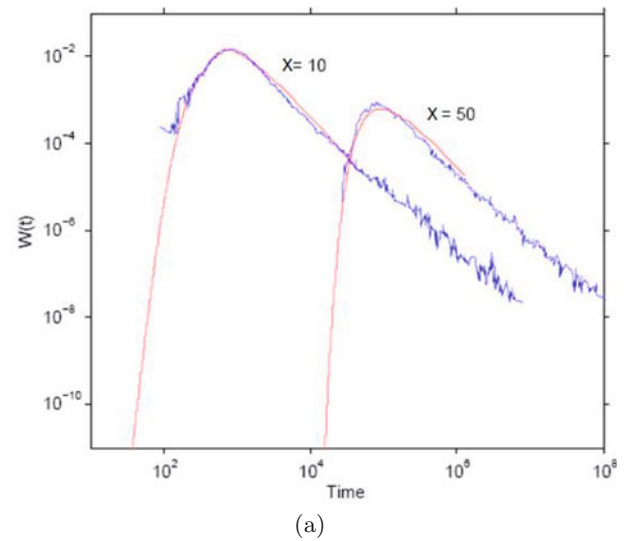


Fig. 5. (a) Comparison of the predicted arrival time distribution, denoted on the axis as $W(t)$, with results from simulations [94]. Three adjustable parameters were employed for the two graphs together; the second curve was generated from the change in x from 10 to 50. Figure is also from [42]. (b) Fit of $W(t)$ to experimental data derived from a breakthrough curve (Figure is from [42]). Data were digitized from reference [16], itself a compilation of “classical” experiments. Fluctuations result from differentiation, a problem partially addressed by simple smoothing techniques.

$t^{-3/2}$ tail (Fig. 5), as often observed in porous media and, particularly in fracture flow experiments (with their two-dimensional flow fields) [91–93]. The comparison with simulations [94] demonstrates that our results at least come very close to the power 1.5 as [94] reported that the slope of their simulated $W(t; x)$ was -1.56 . Their simulations were performed with only structural disorder (system at the percolation threshold, but with no pore-size distribution) and with no input from molecular diffusion.

The agreement with field results [91–93] for the arrival time distribution in fracture flow experiments requires further discussion, as it is more generally believed that the

arrival time distribution is related to diffusive exchange between the rock matrix and the fracture. Consider the following quote from [95] “it is well documented in the literature that matrix diffusion is an important process for retarding solute transport in fractured rock, by allowing for solute storage within the often large void space of the matrix (e.g., [96,97])”. One reason why diffusion into and out of the matrix has been assumed necessary to generate the long-tailed distribution is that the ADE does not do so! Consider the next quote from [95]: “when the advection-dispersion model is used to calibrate against a tracer test conducted in fractured rock with significant matrix diffusion effects, the Peclet number needs to increase to match the highly skewed breakthrough curve with long tailing [98–102]”. Because effects of advection are minimized, effects of diffusion are overemphasized. A scale-effect on the diffusion constant is found, but not understood [95]: “however, it is difficult, if not impossible, to attribute the observed scale-dependence (of the diffusion constant) feature to a particular mechanism or a combination of mechanisms from field observation”.

This discussion demonstrates the greater simplicity as well as generality of our approach. Consider the following quotes from the abstract of [95]: “this trend suggests that the effective matrix diffusion is likely to be statistically scale-dependent. The scale-factor value ranges from 0.5 to 884 for observation scales from 5 m to 2000 m. At a given scale the scale factor varies by two orders of magnitude...” “In addition the surveyed data indicate that field-scale longitudinal dispersivity generally increases with observation scale, which is consistent with previous studies”. In fact this description of the variation and variability of the effective matrix diffusion matches exactly our predictions as well as results for the dispersivity and suggest that the concepts of enhanced diffusion and dispersivity get confused by virtue of the incorrect inference that long-tailed distributions arise only from diffusion into and out of the rock matrix. From [95] again: “the reason for isolating granite is that the lab-scale matrix diffusion coefficient and matrix porosity are usually small for that rock. As shown in Figure 1 it seems that the scale factor of the field-scale matrix diffusion coefficient is not significantly different for granitic rock than for the other types of fractured rock”. Thus the authors do not find a significant dependence on rock type for the enhancement of diffusion. It is interesting that [91–93] find no dependence of the arrival time distribution on molecular diffusion constant either.

The results of [95] for the dispersivity also fit well with the others that we reference, but we do not include their results in the comparison with experiment below because the authors of [95] have manipulated the means to calculate the dispersivity, “second, for the same tracer tests shared in both data sets, our calibrated dispersivity values are smaller than the corresponding values given in Gelhar et al. [18] (see Fig. 4)”. The reason for this recalculation is given above in terms of the increased Peclet number.

Why focus on this paper? Because it exemplifies the risks of basing inferences on properties of the solution of

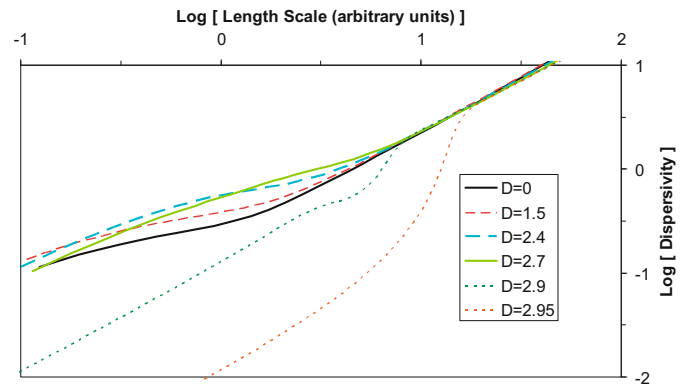


Fig. 6. We demonstrate that for a large range of length values the dispersivity first increases and then decreases for increasing disorder. In the model employed here [76] this is simply accomplished by increasing the fractal dimensionality D from 0 to 2.95. Here $L = 1$

the ADE rather than a more physically based theoretical approach such as ours. Further, [95] and the papers quoted therein represent the typical approach to interpreting experimental data in this field of research.

5.3 Dispersivity

For distances not too different from L the behavior of the dispersivity as a function of length scale is quite non-universal (Fig. 6), but its behavior approaches universality with increasing length scale. This universal behavior is consistent with a slope slightly larger than 1, a result obtained by Sahimi [2,3] many years ago. The universal behavior derived is also nearly identical to a rule of thumb ($\alpha \approx 0.1x$) noted in a review [19] of field data for the dispersivity almost 20 years ago. Note that at large length scales the invasion percolation models typically yield slightly smaller dispersivity values (not shown in detail). Later, when we show data over 10 orders of magnitude of length scale, we will see that these conclusions do not change.

Our prediction is that the dispersivity first increases with increasing disorder of the medium (or heterogeneity), but later diminishes (Figs. 6, 7). The increase is only about a half an order of magnitude. We were originally unaware of this non-monotonic behavior [43,44]. However, it is generally recognized that the dispersivity, at least for relatively small flow heterogeneity, is an increasing function of heterogeneity. We interpret the later diminution as due to the ability of the solutes to find very rapid transport paths, at least at small system length scales, with a consequent higher value of the mean velocity than otherwise expected. Under these conditions we cannot make a definitive statement regarding the deviation between our prediction and the results from reference [103], for which the dispersivity only rises with increasing heterogeneity (albeit more slowly with continued increase in heterogeneity). It is possible that the fact that their results are from three different experiments at different scales means that

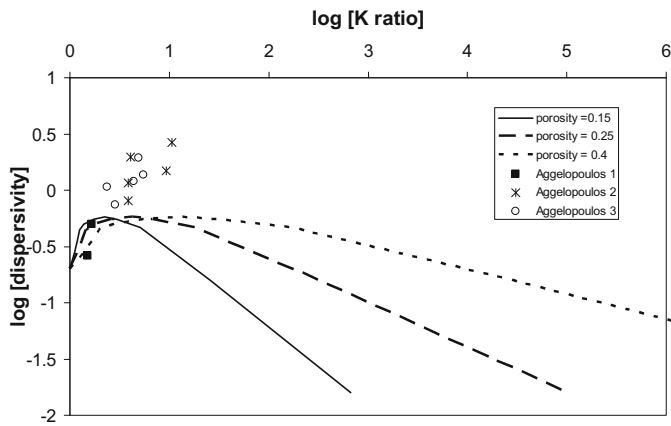


Fig. 7. Comparison of the dependence of the dispersivity on conductivity contrast with experiment [103]. Reference [103] gave results for three different systems, but we have plotted them up together. Note that in none of the systems individually does the dispersivity increase by more than half an order of magnitude, as is also the case for our prediction.

they should be compared with three different theoretical curves, each with different model characteristics (and each exhibiting a peak at a different value of the conductivity contrast). It may be significant that the observed dispersivity only rises by half an order of magnitude in any of the individual systems.

The envelope of predicted dispersivity values coincides remarkably with results from over 1500 experiments [24,33,104–106,108–113] (Fig. 8). In the previous figures we had already chosen the fundamental length scale L to be 1; choice of 1 as 1 meter then led to the agreement shown. We should mention that the “field, fractured” and “field, porous”, as well as lab measurements came from the different references of [24,111]. The other references are described explicitly in the figure caption.

Some authors contend that the scale effect on the dispersivity is not seen in individual experiments, and have constructed experimental configurations that do not exhibit such a scale effect [110]. However, we point out that all of the experimental results from [110] lie within our envelope of predicted values (Fig. 8). Thus it becomes important to document whether the spatial scale effect on the dispersivity is also seen in individual series of experiments. Our results for the 7 data sets we investigated are given in Figure 9. Each is in accord with the overall trend (Tab. 1). Other individual data sets that we investigate separately also show this behavior, as well as most of the individual data sets compiled in [24] and the 680 experiments reported in [20].

Note that the effective slope of 0.83, found by considering all the experiments as a single series, is considerably smaller than the rule of thumb [19], that $\alpha = 0.1x$, which gives a power of 1. The rule of thumb, however, does a better job of predicting the behavior of the dispersivity over the scale of the experiments shown, as can be seen from Figure 9 (and will continue to do better when more length scales are considered). Our approach does even better as

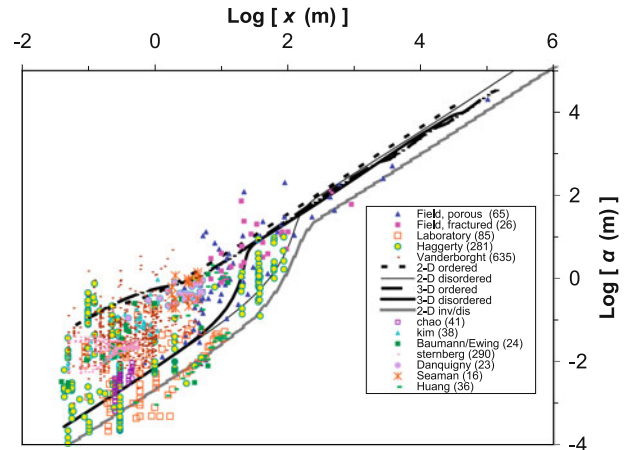


Fig. 8. The length scale dependence of the dispersivity compared with experiment. The axes are both logarithmic. The categories “field, porous” “field, fractured” and laboratory were drawn from references [24,108]. The number in parentheses is the number of data points in that category. Haggerty is from reference [106,107], Vanderborght is from reference [105], Chao is from reference [112], Kim is from reference [111], Baumann/Ewing is combined from reference [113] and from Robert Ewing, Sternberg is from reference [110], Danquigny is from reference [109], Seaman is from reference [104] and Huang is from reference [33]. The designations 2-D, and 3-D refer to the dimensionality of the flow, inv stands for invasion, otherwise the systems are random percolation, “disordered” implies here $D = 2.97$, slightly larger than our original guess [42] of 2.95 to represent a maximum common heterogeneity, “ordered” means actually a much less heterogeneous, but still not homogeneous system, in which the dispersivity takes on approximately its highest values over as large a range of length scales as possible. The curve is also slightly different from our original guess [43] for the result of an ordered system.

Table 1. Scale-dependences of dispersivity in individual experiments.

Data set	# Points	Approximate power	R^2
[112]	41	1.9	0.55
[111]	38	0.99	0.62
[113] ¹	24	0.76	0.82
[109]	23	0.51	0.46
[104]	16	0.88	0.20
[24]	24	1.5	0.95
[24] ²	12	2.5	0.83
Effective values	174	0.83	0.56

¹ The data from reference [113] were combined with data from Ewing that were obtained at a larger length scale.

² The two series from Huang et al. [33] were distinct and could be treated separately.

it is consistent with the tendency of experiments to generate slopes smaller than 1 (3 times out of 3) when their results plot above the rule of thumb and slopes larger than 1 (3 times out of 3) when their results plot below the rule of thumb. The case [113] for which different results are put together at different scales would have raised these statistics to 4 times out of 4 in each case had they been plotted separately, but combining the two demonstrates

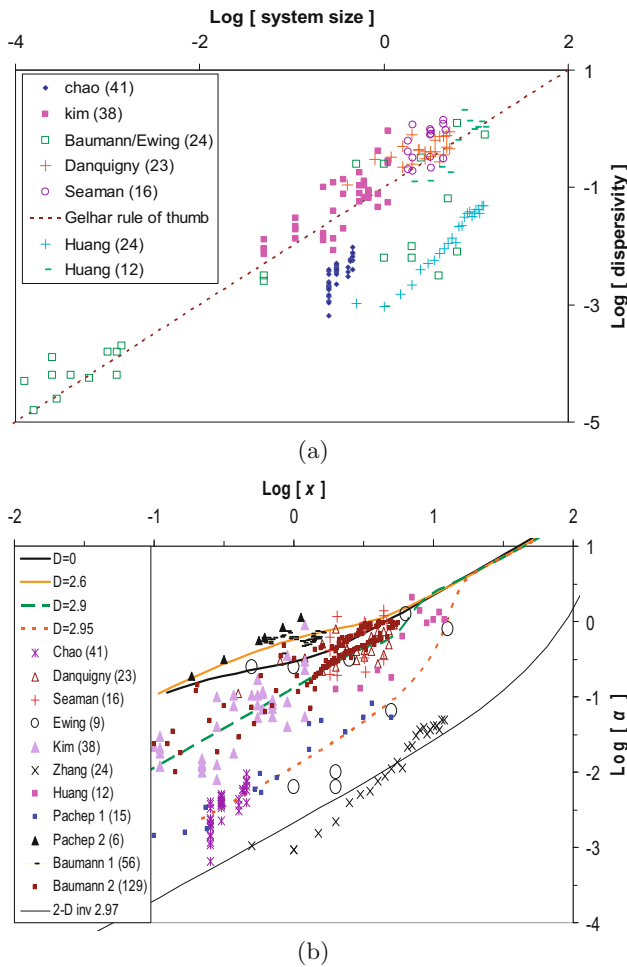


Fig. 9. (a) Comparison of the 7 data sets given in Table 1 with the Gelhar et al. (1992) [19] rule of thumb ($\alpha \approx 0.1x$) for the dispersivity. The rule of thumb is slightly less than the universal portion of the curve predicted here and divides the non-universal portion up relatively evenly on a log scale (as seen in a later figure). Note the tendency of dispersivity data above the rule of thumb to be consistent with a sublinear dependence on the spatial scale while data below the rule of thumb have a superlinear dependence. (b) More explicit representation of the general consistency for data in individual experiments to follow one of our results. Kim is from reference [111], Baumann/Ewing is combined from reference [113] and from Robert Ewing, Sternberg is from reference [110], Danquigny is from reference [109], Seaman is from reference [104] Huang is from reference [33], and Pachepsky is from reference [24]. Zhang can also be found in reference [24]. Both the spatial scale and values of all the data from Baumann had to be multiplied uniformly by numerical constants to translate them to this length and dispersivity scale.

again that putting together unrelated results at different scales tends to reduce the effective slope. On the other hand, concentrating one's attention on too small a range of scales, i.e., field scales, (see the various papers by Neumann) while neglecting smaller scales (such as lab and micromodel scales), allows one to conclude *erroneously* that the power of the dependence of the dispersivity vs. length scale is much larger than 1. Thus our discussion appears

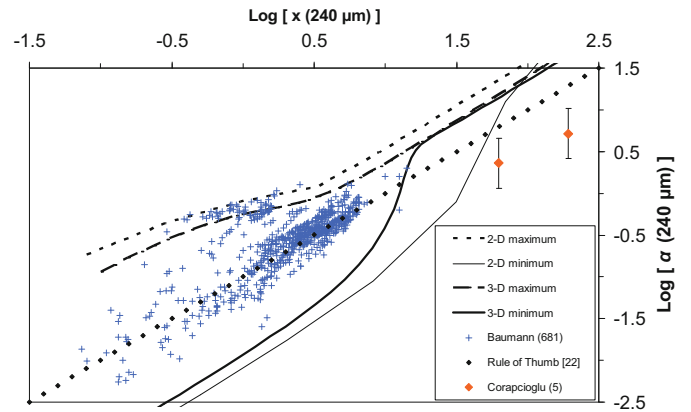


Fig. 10. Comparison of the results of our prediction for the envelope of dispersivity values as a function of spatial scale with results from micromodels [20]. The axes are scaled to a correlation length of 240 μm . Otherwise the curves are identical to those in Figure 8. Here we show the “rule of thumb” together with our predictions.

to resolve a conflict in the literature [114,115], where both slopes less than 1 [114] and greater than one [115] are defended.

As a further check we can apply our predictions to those of micromodels [20,116]. In [20] 680 experiments were performed over scales of a few microns to about 1500 microns and the effective pore separation was about 1 μm . In [116] the pore separation was about a millimeter and experiments were conducted at 6 different length scales, but it was possible to glean with relative certainty only two values of the dispersivity from their text.

In order to validate our predictions we used a range of D values nearly the same (but slightly smaller, stopping at 2.95 instead of 2.97) as for lab and field scales as well as the same value of the critical volume fraction for percolation. Since the largest system size in [20] was on the order of millimeters, one would not expect that a correlation length of 1 m would still be relevant. In fact, we find that changing the correlation length to 220 μm allows our envelope of predicted dispersivity values to match experiment (Fig. 10) even better than at larger scales (99.5% of the experimental values lie within our predicted bounds). Obviously, the correlation length in [116] should be much larger than in those conducted by [20] since their glass bead diameters were approximately 1 mm, almost a factor 1000 greater than the fundamental structure in [20]. If the two data points from [116] are omitted (since for them the dispersivity should not be approaching universal behavior), then our predicted range of values contains nearly 99.8% of experimental values.

We find it useful to put all the data together in Figure 11 (including a few additional data points, such as from [117]). It should be kept in mind that the percolation calculations shown by the envelope of values (for a 1 m correlation length) can not be relevant at scales smaller than about 1 cm and thus do not apply to the micromodel results without a change of scale (as discussed above). Without the change of scale it would appear that

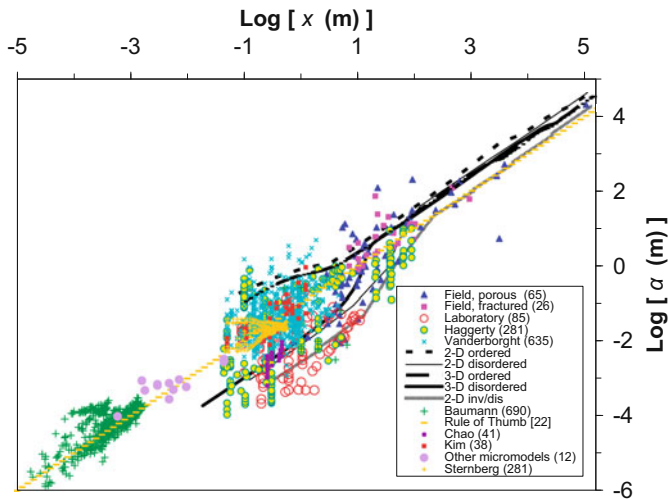


Fig. 11. Comparison of percolation theoretical predictions of the dispersivity as a function of length scale with all the data in both Figures 8 and 10 simultaneously as well as with the “rule of thumb.” The results clearly show that the trend of the data is the same over the entire range of length scales and does not change from a slope of 1.5 to a slope of 1 in the vicinity of 100 m (as suggested in Refs. [13,108]). A slope of 1.5 for length scales below 100 m would lead to dispersivity values of 10^{-8} m at $x = 10^{-4}$ m, instead of the observed values more nearly 10^{-5} m. The data at smaller length scales (mainly [20] and [105]) that show the continuity of the trend consistent with the rule of thumb [19], are not only spread over many orders of magnitude of spatial scale, but they are many (over 1300 data points, more than 10 times the number of data points considered in Ref. [13]).

the single choice of $L = 1$ would suffice to explain experiments conducted over 10 orders of magnitude of length scales, although the predicted variability at small length scales would be larger than observed. But a change of length scale is necessary, while the different values at the greatly different length scales are at least in accord with what theory predicts.

Clearly, when one now examines simultaneously the dispersivity over 10 orders of magnitude of length scale one finds that the asymptotic result from percolation theory, that the dispersivity is roughly linear in the length scale, is still consistent with the rule of thumb [19] and with experiment. Further there is no support for the notion that there is a cross-over in slope from 1.5 for $x < 100$ m to a slope of 1 for $x > 1$ m as represented in [13,108,115], meaning that there is no basis to seek for a cause for such a slope change in a change in sedimentary architecture at a length scale of about 100 m [13,108,115,118]. In fact this apparent change in slope relates to the shape of the envelope of dispersivity values in the approach to universality and can be traced back to a uniformity in experiments (1 m scale) rather than a distinction in media.

Some authors investigate how altering the heterogeneity of the medium produces a variation in the spatial scale dependence of the dispersivity. It should be noted that the controlled modifications of the heterogeneity in these cases

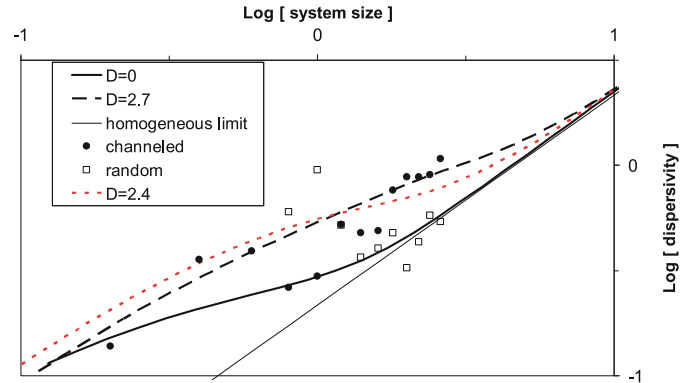


Fig. 12. Comparison of effects on the dispersivity from changing the exponent D with changes in experimental values associated with “channeling” of the flow [109] by correlating the positions of the more permeable regions. The result called “homogeneous limit” was determined visually from the progression of a large number of curves with diminishing D . The trend is consistent with that in Figure 6, but D values even smaller were investigated. Figure 6 stops at $D = 0$ in order to avoid clutter but $D = -2$, for example, continues the linear dependence down another half an order of magnitude in length scales. Note that the equality $r_0 = r_m$ leads to $D = -\infty$, so there is no mathematical limit on D .

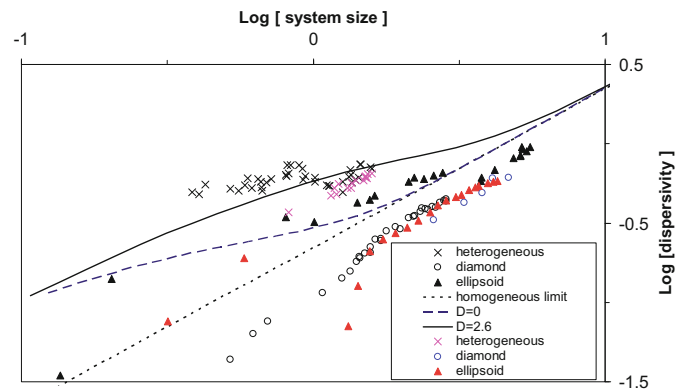


Fig. 13. Comparison of effects on the dispersivity from changing the exponent D with changes in experimental values associated with increased heterogeneity [20] by introducing wider pore-size distributions. Both “diamond” and “ellipsoid” designations are associated with minimal disorder in pore sizes.

are possible because the media are synthetic. As a final check on our ability to predict experiment we investigate this behavior. Consider Figures 12 and 13. In both figures the experimental data reveal an increase in the dispersivity with heterogeneity. In the case of the data from [20], the effective power of the length dependence of the dispersivity also diminishes. While this would also be true for Danquigny et al. [109] data if two of the 9 data points were not included, it is not true if the complete data set is referenced, as can be seen. Of course the two “offending” points also contradict the general tendency for the more disordered systems to have the greater dispersivity.

We should note that in both cases our method failed to predict the precise value of D that would best fit the

data. In comparison with data from [109], our calculation of D (admittedly difficult on account of their considering three different types of media rather than our two types) would lead to $D = 2.4$, whereas the best fit is provided by $D = 2.7$. In the Baumann case [20], our calculation generates $D = 2.8$, while the best fit is provided by $D = 2.6$.

Finally, it is also awkward that in both cases we had to multiply all of our predicted dispersivity values by the numerical factor 2.39, in order to provide the consistency. Of course part of the problem is that our treatment does not cover all the possible inputs into dispersivity as we note that systematic variation occurs with particle diameter and chemical composition (e.g., [20]) that we never address. We also suspect that these failures in precision encountered through such detailed comparison are due at least partly to the fact that, particularly in engineered media, the fractal model for the pore space (or composite medium) is not appropriate. Note that in neither case does the best fit D (2.6 and 2.7) correspond to a strongly heterogeneous material; these values correspond to hydraulic conductivity contrasts (i.e., K_m/K_0) a little over an order of magnitude (in case that the more conductive portion of the medium has volume fraction 40%) or as little as a half an order of magnitude (in case the more conductive portion of the medium has volume fraction 30%). In lab and core samples of porous media, typical D values are 2.8 or higher [40], with values as high as 2.95 common, although such high values of D occur mostly for reasons that the porosity is small (less than a typical value of 40%). Nevertheless, $D = 2.93$ for effective porosity of 40% corresponds to a hydraulic conductivity contrast of 4×10^6 .

These observations suggest that the range of heterogeneity investigated in typical experiments on synthetic media may be inadequate on which to base inferences about nature. This is particularly true when such media as glass beads are considered, for which the pore-size distribution is nearly monodisperse. In particular, contrasts in their pore sizes are frequently no more than 10% to 50%. Even at 50%, the conductivity contrast is $(1.5)^2$, or about a third of an order of magnitude.

5.4 Dispersion coefficient

For small times we find that the dispersion coefficient of sufficiently heterogeneous systems is roughly proportional to a small power of the time, in accord with general experimental results and possibly predictive as well [44]. We do not discuss this further in this particular paper, but it appears that a reasonably good job of predicting the temporal dependence of the dispersion coefficient in the Borden aquifer in Ontario Canada was made without any knowledge of the properties of the subsurface and with no adjustable parameters [44]. Values for the correlation length exponent and the mass fractal dimensionality of the backbone were chosen appropriate for three-dimensional flow under conditions for random percolation. For larger times our calculation yields a diminution of the dispersion

coefficient with increasing time [44], except for 2-D invasion percolation with large disorder. At the time the crossover to diminishing dispersion coefficient occurs, the spatial dependence of the dispersivity becomes universal (all the different models generate essentially the same curve).

We still do not know whether this is a physically viable solution or not, since we have not yet verified whether it violates the central limit theorem (CLT). If it does violate the CLT, but replacement of the derived dependence by a constant (in accord with the CLT) does not affect the spatial dependence of the dispersivity, then we would have a very interesting result. In particular, the dispersion coefficient would then cross over to a Gaussian limit in very large system sizes, but the dispersivity would continue to rise, albeit also in a universal fashion.

6 Diffusion

6.1 Incorporating effects of diffusion

We treat the effects of diffusion explicitly at the pore scale [43]. Equation (1) is, at the pore scale, consistent with treatments based on the Peclet number, P_e [70], which is the ratio of the time it would take a particle to diffuse out of a pore of radius r to the time it takes for it to be advected through a pore of length r . This calculation [1] gives,

$$P_e = \frac{r^2/D_m}{r/v} = \frac{rv}{D_n}. \quad (8)$$

We find an approximation to the probability, f , that a particle diffuses off a given path characterized by a given flux at some particular pore with radius r (and length l proportional to r). Since the diffusion term in equation (1) (valid at the pore scale!) derives from the idea that probability fluxes are proportional to concentration gradients, probabilities of escape per unit time for individual particles have been assumed constant. This implies that, at least for large velocities and small advection times, the probability that a particle can exit a given pore by diffusion is the ratio of the advection time, t_A to the molecular diffusion time, which is the inverse of the Peclet number above. Then the probability, f_i , that a given particle leaves pore i by diffusion is (also found in [119]),

$$f_i \propto \frac{t_A}{t_D} = \frac{1}{P_e} = \frac{D_m r}{Q}. \quad (9)$$

Here Q is the fluid mass flux through a pore. A compatible result that the time for escape from a dead-end is proportional to P_e was found in [120], as transition rates and survival times are inverses of each other. The final equality arises from the identity $Q = Av \propto r^2 v$. The assumed proportionality of pore length and radius makes $A/l \propto r$. On a path with conserved Q , the pore with the largest radius provides the best chance to escape on account of its smallest value of P_e . The probability, P , that the particle remains on the flow path at a given pore is $1 - f$. In order

to stay on the given flow path it must stay on at every opportunity, which generates a product of $1 - f$ over all the pores along the flow path. If fluid velocities are large enough, f is so small that we can use the relationship $\exp(-dx) \approx 1 - dx$ to transform the product

$$\prod_i (1 - f_i) \quad (10)$$

to

$$\exp \left[- \sum_i f_i \right] = \exp \left[- \sum_i \frac{1}{P_e} \right]. \quad (11)$$

We can simplify the sum inside the exponential by representing it as the product of a typical value P_{ec}^{-1} of P_e^{-1} and a number corresponding to the frequency of opportunities to “jump” to another flow path. This number is essentially the number of correlation lengths, L , traversed, and can be found by taking the product of the number of pores visited on a path $(x/r_m)^{d_{min}} |1 - (g/g_c)^{1-D/3}|^{-d_{min}}$ and the fraction of pores that provide close contact with other paths r_m/L .

$$\exp \left[- \frac{r_m}{L} \left(\frac{x}{r_m} \right)^{d_{min}} \left| \frac{1}{\left(\frac{g}{g_c} \right)^{1-D/3} - 1} \right|^{d_{min}} \left(\frac{1}{P_{ec}} \right) \right]. \quad (12)$$

We chose the scaling exponent d_{min} that is the fractal dimensionality of the optimal path [84]. This choice was made because we assumed that the spatial tortuosity factor is relevant to counting the number of opportunities for diffusion-induced transitions off the path. Perhaps the mass fractal dimensionality, D_b would have been a better choice here as well, but the answer to this question is as yet unknown. In addition to the obvious tendency for factor (11) to reduce the contribution of highly tortuous paths (with g near g_c) to large travel times, it also reduces the tendency of very slow paths (with small controlling g and thus small P_e) to contribute to large travel times. Since there has been some question as to which of these cases was most important to incorporate into dispersion calculations [121–123], it is rewarding to find out that our calculation scheme accounts for both automatically. The result from procedure D in Section 4.3.1 must now be multiplied by result (11) to generate,

$$W(t)dt = \frac{gW(g)}{dt/dg} \times \exp \left[- \frac{r_m}{L} \left(\frac{x}{r_m} \right)^{d_f} \left| \frac{1}{\left(\frac{g}{g_c} \right)^{1-D/3} - 1} \right|^{d_f} \left(\frac{1}{P_{ec}} \right) \right]. \quad (13)$$

The calculations in [43] stopped at this point. For the purposes of investigating changes in dispersion at constant velocity due to variations in the molecular diffusion constant, that was appropriate. However, the Peclet number can also change due to changes in velocity for a given molecular diffusion constant. While these two cases are typically

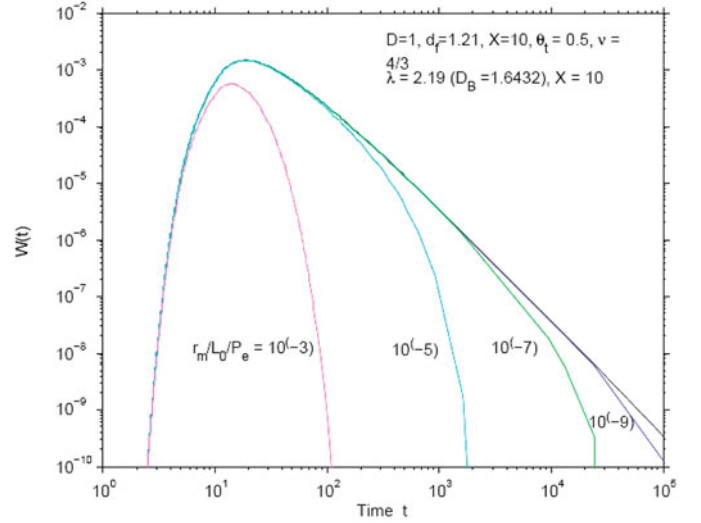


Fig. 14. Shows predicted changes in the arrival time distribution due to increasing effects of diffusion (diminishing Peclet number). The ratio of lengths and Peclet number diminishes as the Peclet number increases. The listed parameters are valid for 2-D invasion percolation systems with critical volume fraction 1/2 for example, and the appropriate values [60] for the mass fractal dimensionalities of the backbone (1.6432), optimal paths (1.21) and the exponent of the correlation length (4/3) respectively. The system size was 10.

treated interchangeably, they are not interchangeable in the present format.

An additional effect of increasing velocities is that solute particles are advected downstream faster, meaning that large clusters of interconnected resistances become important at smaller times. This effect is easily treated simply by adding a factor of $1/P_e$ to the expression (Eq. (7)) for $t(g)$. This change has no effect on the representation of dispersivity as a function of distance, but it brings the peak in the dispersion coefficient (or crossover to universal behavior, if that should be the case) to smaller times. We will see below what the result of this distinction is.

6.2 Effects of diffusion on the predicted dispersion coefficient and dispersivity

The most important effects of diffusion are that the heavy tails in spatial and temporal distributions disappear (Fig. 14) and, as a consequence, Gaussian spreading is eventually recovered [15,16,124,125]. As seen the time at which the effects of diffusion set on diminishes with diminishing Peclet number. As a consequence, the rises in the value of the dispersion coefficient with increasing time and of the dispersivity with increasing scale are terminated. In the case of the dispersion coefficient (Fig. 15), the effects are not spectacular, since our theory does not generate an indefinite increase with increasing time anyway. But if diffusion is relevant, at some spatial scale the value of the dispersivity must level off (Fig. 16), consistent with Gaussian spreading. This result is simply not seen in

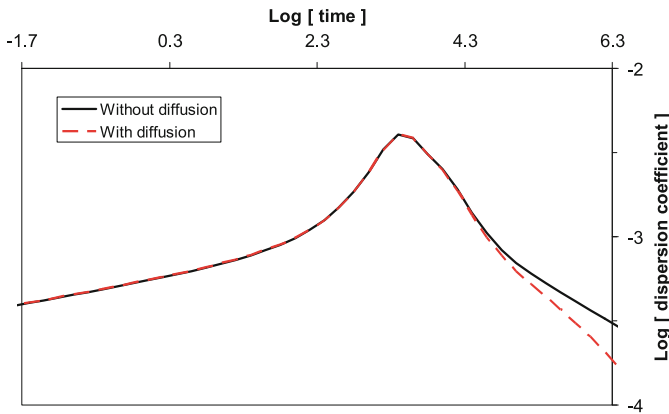


Fig. 15. Shows effects of diffusion on the dispersion coefficient (for large Peclet number). It is not clear whether the values at times greater than the peak time are valid. It is possible that a diminishing dispersion coefficient in the long-time limit violates the central limit theorem (CLT) because the variance then does not increase as fast as linear in the time. The result arises from the fractal nature of large clusters near the percolation threshold and the transformation (Eq. (7)) $t \approx x^{D_b}$, so that even though the dispersivity still rises rapidly, the transit of the particles is so slow in time that the dispersion coefficient diminishes. In a truly fractal medium there is no such restriction from the CLT, but our treatment is of fractal flow paths through a (disordered) Euclidean medium.

the experiments compiled (Fig. 11), with the exception possibly of one data point. As a consequence we conclude that the effects of diffusion, at least at large spatial scales (upwards of 1 m), are negligible. While many physicists might find this reasonable, this is quite an unusual conclusion among scientists active in explaining properties of porous media.

Consider the dependence of the dispersion coefficient at a given time on Peclet number. It turns out that either case (changing velocity or changing diffusion constant) produces slightly superlinear scaling of the dispersion coefficient on Peclet number for values $1 < P_e < 100$, (Figs. 17 and 18) in agreement with a number of authors [121–123,126–128]. Figure 17, for changing velocity, is new, whereas Figure 18, for the case of changing diffusion, is from [43]. We should point out that, in contrast to Figure 17, Figure 18 shows the dependence of the maximum value of $D_l(t)$ on P_e rather than D_l at a fixed time. For small values of P_e , (less than 100) this maximum value of $D_l(t)$ occurs at the first time step, and the two representations are equivalent. But, in those cases for which $D_l(t)$ has a peak (every case except for two-dimensional invasion percolation), the peak's existence tends to introduce a horizontal asymptote to the graph of $D_l(P_e)$ at large P_e values.

In Figure 17 the plot is for four different times (and parameters representative of some rather disordered media). As time increases the value of the dispersion coefficient for the lowest Peclet number diminishes and the initial slope of $D_l(P_e)$ vs. P_e increases. The range of Peclet numbers plotted is from 1 to 10000. The straight line has slope of

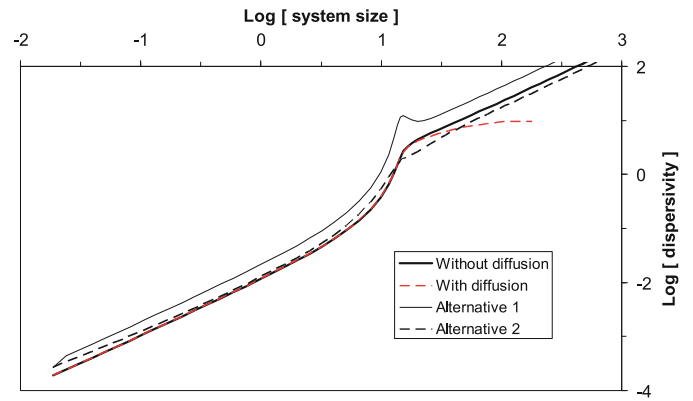


Fig. 16. Shows effects of diffusion on the dispersivity. Alternative 1 and Alternative 2 are slightly different ways to calculate the dispersivity, which is typically calculated using the ratio of the dispersivity and the solute velocity, instead of our method of dividing the variance by the mean solute distance. While these two methods may sound identical, they need not be when the solute velocity is a diminishing function of time. This shows that some of the data points that lie outside our range of predicted values in Figure 8 may simply have been calculated in a different manner. An alternative hypothesis could be that it is inadequate to consider a distribution of local conductances which is monomodal and a bimodal distribution is required.

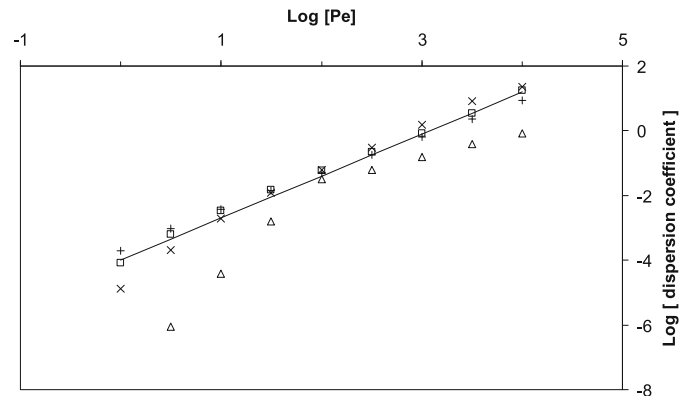


Fig. 17. Shows the dependence of the calculated dispersion coefficient on Peclet number for four different times. The trend is to smaller dispersion coefficients at longer time scales because of the peak in the dispersion coefficient as seen in Figure 15.

1.3. Thus one can see that, at least for the three small time values, the result is a superlinear power though with slope a little larger than the commonly reported value of 1.2 [121–123,126–128]. For the larger value of the time, systematic increase of the Peclet number eventually brings the system past the peak in the dispersion coefficient as a function of time, leading to a more complicated (and unverified) dependence of the dispersion coefficient on Peclet number. But for the three smaller values of the time one can detect a diminution of the slope of $D_l(P_e)$ vs. P_e , as noted also in [121–123,126–128].

Figure 18 and its insert show, as reported in [43], that our calculations are consistent with $D_l(t) \propto P_e^\delta$. Allowing

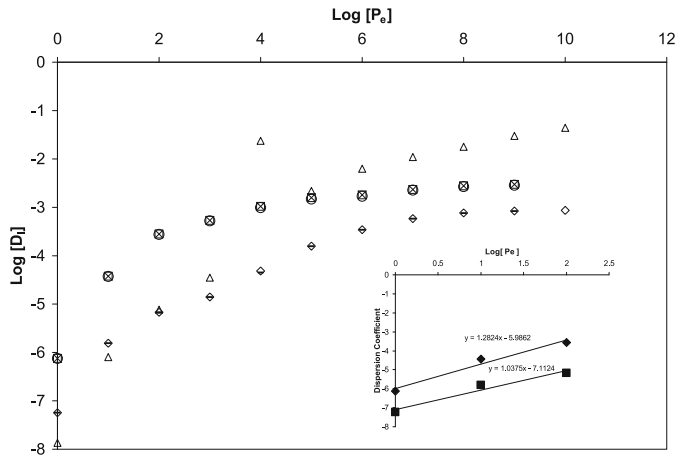


Fig. 18. Scaling of D_l with P_e for highly disordered media (largest pore sizes thousands of times larger than the smallest). Note that the value of D_l for infinite P_e is reached only after 8 orders of magnitude increase of P_e (for five systems), while D_l continues to rise in the sixth. Also the typical increase in D_l here is about three and a half orders of magnitude, at least two orders of magnitude more than for nearly ordered media [43] (with largest pore size less than 50% larger than the smallest). Open triangles 2-D invasion, $d_{min} = 1.22$, open circles 3-D invasion, $d_{min} = 1.37$, open diamonds 2-D invasion, $d_{min} = 1.13$, dashes 2-D random, $d_{min} = 1.13$, crosses 3-D random, $d_{min} = 1.46$, open squares 3-D random, $d_{min} = 1.37$. The inset shows the Excel value of the slope for two cases.

Excel to pick the slope in the range $1 < P_e < 100$ lead to values $1 < \delta < 1.38$, with an average value of nearly 1.2 for the 4 cases considered (two and three dimensions, random and invasion percolation) as long as the medium could be considered disordered. For ordered media, our calculations did not reproduce the observed scaling.

Only when the increase in P_e is due to increasing velocity and at smaller times (or for the case of invasion percolation in two dimensions when the increase is due to diminishing diffusion constant) do we see the tendency to generate an additional regime for larger P_e where the slope diminishes to values more nearly equal to 1.

7 Dependence of typical transit times on length

In references [67,129], early publications establishing the ability of the CTRW to model electronic transport in disordered semiconductors, the implications of the power-law tails of the arrival time distributions on typical particle times of transit of systems of a given length were discussed. In those works it was shown that observed power-law tailing in electron arrival time distributions could be used to predict the power of the dependence of the typical transit time on system length. Our equation (7), with its dependence of the typical transport time on the transport distance raised to a power equal to the fractal dimensionality of the backbone, directly implies the observed scaling

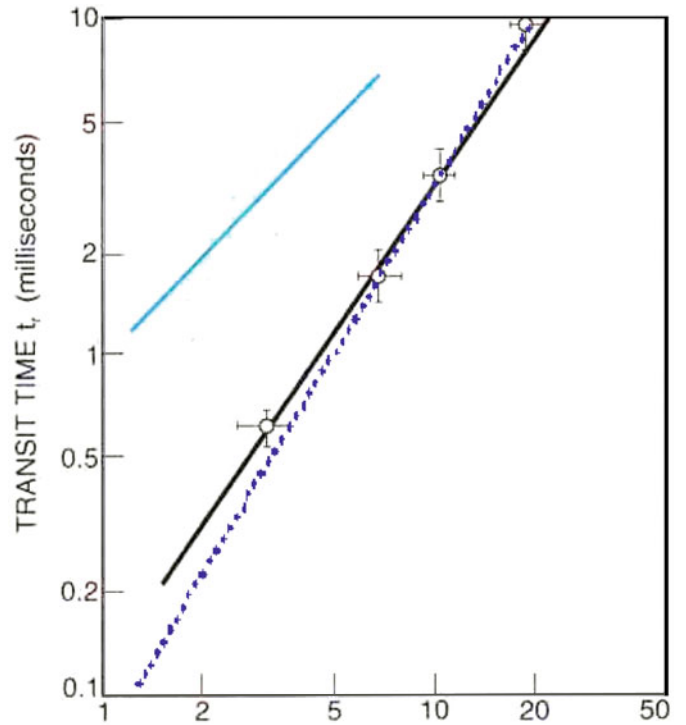


Fig. 19. The dependence of the typical travel time, t , on system length. The data are circles, the separate blue line is a linear dependence, the solid line through the data is the prediction of CTRW based on the observed time-dependent photocurrent, and the dotted line is the prediction from percolation theory [85], that $t \approx x^{D_b}$, where $D_b = 1.9$ is the fractal dimensionality of the backbone in three dimensional flow problems [60]. Note that the CTRW and percolation predictions are roughly equally successful over the set of four data points and nearly two orders of magnitude of time. In particular, the CTRW prediction misses at the highest point, while percolation misses at the lowest point. But because the CTRW exponent was obtained from experiment, while percolation delivers a prediction from theory, the possibility emerges that use of CTRW can be informed by percolation theory.

of time with length as seen in Figure 19 (modified from Ref. [129]).

Power-law dependences of transit time on system length with similar, but not identical, numerical values of the powers were observed in many systems (see Tab. 2) The average value of these powers is 1.81, about 5% different from the prediction of 1.9 (the fractal dimensionality, D_b , of the backbone) from random percolation theory in three dimensions. While a spread in the reported values of this power certainly exists, this variability may be, at least judging from Figure 19, partly due to experimental uncertainty compounded by having only few data points. Besides, $D_b = 1.64$ for two-dimensional conduction or flow, while values of 1.46 are relevant in invasion percolation in three dimensions and 1.22 for invasion percolation in two dimensions [60]. Still the value for D_b for random percolation in three dimensions appears to be reasonably in accord with a wide range of the data. And because the CTRW exponent was obtained from experiment, while

Table 2. Reported values of the exponent describing the power-law dependence of travel time on length.

Power	Reference	Material
1.67	Pfister and Griffiths [130]	Carbazole polymers
1.72	Pfister and Griffiths [130]	Carbazole polymers
2.1	Pfister [131]	As ₂ Se ₃
2	Tiedje [132]	a-Si:H
2.2	Scher and Montroll [67]	Not given
1.91	Pfister [133]	a-Se
1.86	Pfister [133]	a-Se
1.61	Bos et al. [134]	Polyvinyl carbazole
1.82	Pfister and Scher [135]	Not given

Note that transport through localized states, the presumed cause of the dispersive transport [67], is restricted to the (2) transverse dimensions in polymer chains, consistent with the observed exponents near 1.64 in those systems.

percolation delivers a prediction from theory, the possibility emerges that use of CTRW can be informed by percolation theory.

8 Summary and conclusions

The traditionally used advection dispersion equation (ADE), generally consistent with Gaussian spreading of contaminant plumes, is not typically consistent with experiment or observation. Solved stochastically for a heterogeneous medium it preserves the Gaussian spreading in the limit of large transport distances or times, though if heterogeneity that evolves continuously with increasing spatial scale is invoked, the asymptotic Gaussian limit may be deferred indefinitely. Nevertheless, in its currently published version, even this modification of the ADE does not properly describe experimental data over the entire range of length scales investigated, in which a linear relationship of dispersivity to transport distance is observed (Figs. 8–11). This linear proportionality was described nearly two decades ago already in the hydrology literature [19], and even longer ago in a critical early paper [67] in the development of the CTRW, and published [2,3] over 20 years ago in a paper using scaling arguments of percolation theory for the asymptotic large length regime. We emphasize that only the papers using scaling arguments of percolation theory restrict their treatment to the critical cluster. Our approach uses all possible clusters according to the probability of their occurrence and generates a significant region of non-universal behavior at smaller length scales.

A number of alternate means to generate, more or less accurately, the spatio-temporal evolution of solute plumes have been given. Most of these descriptions are known [136,137] to be subsets of the general framework referred to as the Continuous Time Random Walk (CTRW). Despite its generality, the CTRW is not presently a predictive theoretical approach as it (and especially its asymptotic ‘fractional derivatives’ version [136,137]) critically needs a set of parameters, starting with the order of the

fractional derivatives, to explain observed data. In specific cases, these parameters and functions may be supplied by other means [138], such as simulations [126]. But our approach is to use a procedure based on microscopic physics to derive analytically the spatial and temporal distributions of solute particles carried passively through a porous medium for which the relevant numerical parameters are specified by theory. Especially in light of the comparison of our predictions with experiment, these results should provide a theoretical basis for choice of appropriate inputs to CTRW.

Our theoretical predictions for dispersion in porous media derive from the logical application of concepts of percolation theory to systems with wide ranges of local conductance values. The framework is based on the cluster statistics of percolation theory in the language of critical path analysis, a combination which allows direct calculation of the probability that a system of a given length is spanned by an interconnected path (backbone of a percolation cluster) with an arbitrary smallest value of the conductance. Use then of the knowledge of the length scale and closeness to the percolation threshold dependences of the time of particle transit of such a cluster allows calculation of the arrival time distribution of solute particles crossing such a system. An analogous calculation allowed the determination of the spatial distribution of solute particles at an arbitrary time.

When we compared with experiment our theoretical predictions for the dispersivity that were obtained by neglecting effects of diffusion, our overall conclusion was that we had captured the most important physics guiding the results, but that some important influences on dispersion may have been omitted. Nevertheless, molecular diffusion, or any analog to it, appeared to have essentially no role in the values of the dispersivity over a wide range of length scales. Since theoretical arguments clearly establish the relevance of diffusion at sufficiently small flow velocities, we can only conclude that, in most of the nearly 2200 experiments we considered, the actual flow velocities were too large, or diffusion constants too low, for diffusion to have been relevant.

Some uncertainties remain.

As in [43,44], we cannot yet say whether our calculated result of a diminishing dispersion coefficient at long time scales contradicts experiment, or even the central limit theorem. Further research needs to be done in this area.

A second persistent uncertainty is whether it is sufficient to consider only a typical cluster crossing time. At first glance it would appear to be necessary to consider the entire distribution of such times [84,119]. However, we have considered clusters governed by all different conductances individually and the possibility exists that utilizing these two means of counting simultaneously could lead to overcounting the possible arrival paths and thus overestimating the width of the arrival time distribution. One could then assert that our predictions could never be made consistent with pure percolation scaling in the limit that the disorder is only topological, not geometrical (e.g., pore size distribution). But our results appear to do

a reasonable job (Fig. 5a) of predicting the arrival time distribution for purely topological disorder in two dimensions [94]. The answer to this question remains open.

Finally, although we have had some success in incorporating the effects of diffusion on dispersion, it is clear to us that this theoretical treatment can only be considered asymptotic, even if it appears to be accurate for Peclet numbers as small as $P_e = 1$ (where transport by molecular diffusion over the spatial scale of a single pore is equally quick as that by advection).

We believe that we have given a strong case for abandoning use of the continuum mechanics derived advection diffusion equation (ADE), while, outside of percolation theoretical techniques, we have not found any support for any of the other alternatives proposed for it, other than formal descriptions (CTRW) that may need percolation theoretical results to guide the choice of the relevant parameters.

In greater detail we have found (in the absence of diffusion):

(1) Our predictions for the functional form of the solute arrival time distributions are in accord with a number of experiments. In particular reference [42] already demonstrated their general consistency with the classic experiments considered in [16] as well as with simulations performed in [94]. Here we have argued that they are consistent also with the long-tail arrival time distributions in fracture flow experiments that have been traditionally interpreted in terms of a completely different mechanism. Finally, the predicted solute arrival time distribution even appears to follow the same behavior [42] as found in clogging time distributions [139,140].

(2) Our predictions for the system length dependence of the dispersivity (slightly superlinear in x) are verified here by comparison with approximately 2200 experiments over 10 orders of magnitude of length scales (from 10 μm to 100 km), both individually and collectively. These experiments include micromodels, lab scales, field scales and media that are both porous and fractured, all in precisely the same framework. The nearly linear behavior was also claimed [67] to be characteristic of non-equilibrium charge transport in disordered semiconductors.

(3) Our prediction for the time dependence of the dispersion coefficient in 3-D and for short time scales (a small positive power of the time) appear to be in agreement [44] with experiments [141–144] performed at the Borden aquifer. The predicted power for heterogeneous systems in 2-D was found [44] to be identical to that generated by simulations for a regular network and with a log-normal distribution of conductances [145].

(4) Results (2) and (3) combined imply that the solute velocity is a diminishing function of the time, as can be seen from equation (7), in which arrival times, t , are super-linear in distance, x . While this result is clearly established in disordered semiconductors (see Sect. 7), we have as yet only one reference [146] that allows a test of this suggestion in solute transport in porous media. In particular, from depths of 50 cm to 100 cm, the longitudinal dispersivity increased from 1.2 cm to 2.5 cm, consistent with a

linear dependence of dispersivity on travel distance [146], whereas the apparent solute velocity diminished [146] by a factor nearly 2, as we predicted. In addition our result implies that, especially over longer distances, the mean solute velocity must be less than the mean flow velocity, as claimed in [147].

(5) Our predictions for the width of the distribution of dispersivity values as a function of length scale are verified separately for at least two widely differing ranges of length scales.

(6) Our predictions for the heterogeneity dependence of the dispersivity at small magnitudes of the heterogeneity are generally in accord with the data (Figs. 7, 12, 13), but at higher values of the hydraulic conductivity contrast we may underestimate the dispersivity. On the other hand comparison with the large data sets (Figs. 9–11) seems to indicate that we have found the explanation for the lower bounds on the dispersivity as a function of length scale by relating them to the highest commonly found magnitudes of heterogeneity.

Further, our simplest approach to account for diffusion appears to generate scaling of the dispersion coefficient with Peclet number in accord with known theory and experiment.

Consequently, we conclude that we have at least found the appropriate basis for treating solute dispersion mediated by flow in porous media. It is also clear that our theory will benefit particularly from two further improvements: (1) a better understanding of the long-time behavior of the dispersion coefficient and the potential discrepancy between our derivation and the central limit theorem [43,44], (2) a better treatment of diffusion than our initial asymptotic attempt.

We have found no better explanation for the fact that the vast majority of data for the dispersivity at length scales exceeding centimeters can be explained with a single choice of the correlation length of 1 m than that this length is determined by the experimenter [44]. Such an influence can be deduced to be mediated by the choice of the initial volume of solute, which may vary over an order or two of magnitude in such experiments, but not so much that its cube root (which gives its linear dimension) varies a great deal on a logarithmic scale. In [44] we were able to show that in the specific case of the experiments on the Borden aquifer [141–144] the correlation length was indeed on the order of 10 times the dimensions of the relevant heterogeneity as predicted already in [75]. This was possible because other authors [148,149] had already determined the size of the sedimentary deposits responsible for the primary influence on the dispersion.

Our theory, which treats only a single scale of heterogeneity, develops a dispersivity which continues to rise without bounds as the scale of the experiment increases. The width of the distribution of dispersivity values eventually tends towards zero at very large scales (universal behavior). In order for this conclusion to be contradicted, we must not only have many scales of heterogeneity, but initial conditions that were a function of spatial scale. Thus, it is not the continued rise of the dispersivity that indicates

the simultaneous relevance of many scales of heterogeneity, but the continued wide range of dispersivity values. Of course such a scenario is possible, but our investigation of the data does not yet support it. Thus we conclude that a considerable amount of attention has been directed in vain to the problem of how to treat media with many scales of variability. The only scales that need to be addressed are those immediately larger than the one determined by the initial solute volume. Of course this conclusion was based on the assumption that heterogeneity of all scales exists in natural porous media. Nevertheless, it is not possible to draw the correct conclusions if the theoretical approach is inadequate.

The authors are indebted to Prof. Haggerty, Prof. Baumann, and Dr. Vanderborght for sharing original data (making digitization unnecessary). Discussions with Hans Herrmann and the input of the referees are also gratefully acknowledged. This research was supported by NSF grants EAR 0810186 and EAR 0911482.

References

1. J. Bear, *Dynamics of Fluids in Porous Media* (American Elsevier Publishing Co. Inc., New York, 1972)
2. M. Sahimi, A.O. Imdakm, *J. Phys. A* **21**, 3833 (1988)
3. M. Sahimi, A.O. Imdakm, *Phys. Rev. Lett.* **66**, 1169 (1988)
4. B. Berkowitz, H. Scher, *Water Resour. Res.* **31**, 161 (1995)
5. M. Hunter, P. Callaghan, *Phys. Rev. Lett.* **99**, 210602 (2007)
6. F.A.L. Dullien, *Porous Media: Fluid Transport and Pore Structure* (Academic Press, San Diego, CA, 1992)
7. N. Martys, *J. Chromatogr. A* **707**, 35 (1995)
8. D. Dan, C. Mueller, K. Chen, J. Glazier, *Phys. Rev. E* **72**, 041909 (2005)
9. G. Gibson, C. Gilligan, A. Kleczkowski, *Proc. R. Soc. Lond. B Biol. Sci.* **266**, 1743 (1999)
10. J.T. Truscott, C.A. Gilligan, *Proc. Natl. Acad. Sci. USA* **100**, 9067 (2003)
11. S. Karimian, A. Straatman, *J. Heat Transfer* **131**, 052602 (2009)
12. M. Agop, P. Nica, P. Ioannou, A. Antici, V. Paun, *Eur. Phys. J. D* **49**, 239 (2008)
13. S.P. Neuman, *Water Resour. Res.* **26**, 1749 (1990)
14. B. Berkowitz, H. Scher, S.E. Silliman, *Water Resour. Res.* **36**, 149 (2000)
15. G. Margolin, B. Berkowitz, *J. Phys. Chem. B* **104**, 3942 (2000)
16. A. Cortis, B. Berkowitz, *Soil. Sci. Soc. Am. J.* **68**, 1539 (2004)
17. M. Levy, B. Berkowitz, *J. Contam. Hydrol.* **64**, 203 (2003)
18. A. Arya, T.A. Hewett, R.G. Larson, L.W. Lake, *SPE Reserv. Eng.* **3**, 139 (1988)
19. L.W. Gelhar, C. Welty, K.R. Rehfeldt, *Water Resour. Res.* **28**, 1955 (1992)
20. T. Baumann, L. Toops, R. Niessner, *Water Res.* **44**, 1246 (2010)
21. W.A. Jury, Solute transport and dispersion, in *Flow and transport in the natural environment: advances and applications*, edited by W.L. Steffen, O.T. Denmead (Springer Verlag, Berlin, 1988), pp. 1–16
22. L. Zhou, H.M. Selim, *Advances in Agronomy* **80**, 223 (2003)
23. T.R. Ellsworth, P.J. Shouse, T.H. Scaggs, J.A. Jobes, J. Fargerlund, *Soil Sci. Soc. Am. J.* **60**, 397 (1996)
24. Y. Pachepsky, D. Benson, W. Rawls, *Soil Sci. Soc. Am. J.* **64**, 1234 (2000)
25. A.E. Scheidegger, *An evaluation of the accuracy of the diffusivity equation for describing miscible displacement in porous media*, in *Proc. Theory of Fluid Flow in Porous Media Conf.* (Univ Oklahoma, 1959), pp. 101–116
26. M.M. Meerschaert, J. Mortensen, S.W. Wheatcraft, *Physica A* **367**, 181 (2006)
27. R. Sanchez, B.A. Carreras, B.P. van Milligen, *Phys. Rev. E* **71**, 011111 (2005)
28. N. Krepyshva, L. Di Pietro, M.C. Neel, *Phys. Rev. E* **73**, 021104 (2006)
29. A. Zoia, A. Rosso, M. Kardar, *Phys. Rev. E* **76**, 021116 (2007)
30. X.X. Zhang et al., *Water Resour. Res.* **41**, W07029 (2005)
31. Y. Zhang et al., *Water Resour. Res.* **43**, W05439 (2007)
32. M.V. Kohlbecker, S.W. Wheatcraft, M.M. Meerschaert, *Water Resour. Res.* **42**, W04411 (2006)
33. G. Huang, Q. Huang, H. Zhan, *J. Contam. Hydrol.* **85**, 53 (2006)
34. K. Kilse, V.C. Tidwell, S.A. McKenna, *Adv. Water Res.* **31**, 1731 (2008)
35. C. Knudby, *Adv. Water Res.* **28**, 405 (2005), doi:10.1016/j.adwatres.2004.09.011
36. M. Willman, J. Carreras, X. Sanchez-Villa, *Water Resour. Res.* **44**, W12437 (2008)
37. E. LaBolle, G. Fogge, *Water Resour. Res.* **37**, 83 (2001)
38. A. Western, G. Bloeschl, R. Grayson, *Transp. Porous Media* **42**, 155 (2001)
39. M. Sahimi, *Applications of Percolation Theory* (Taylor & Francis, London, 1994)
40. A.G. Hunt, R.P. Ewing, *Percolation theory for flow in porous media*, *Lecture Notes in Physics*, 2nd edn. (Springer, Berlin, 2009)
41. A.G. Hunt, *Complexity* **15**, 13 (2009)
42. A.G. Hunt, T.E. Skinner, *Phil. Mag.* **88**, 2921 (2008)
43. A.G. Hunt, T.E. Skinner, *J. Stat. Phys.* **140**, 544 (2010)
44. A.G. Hunt, T.E. Skinner, *Complexity* (2010), doi:10.1002/cplx.20322
45. L.W. Gelhar, *Water Resour. Res.* **22**, 1358 (1986)
46. *Subsurface Flow and Transport: A Stochastic Approach*, edited by G. Dagan, S.P. Neuman (Cambridge University Press, Cambridge, UK, 1997)
47. C.L. Winter, D.M. Tartakovsky, A. Guadagnini, *Surveys Geophys.* **24**, 81 (2003)
48. C. Miller, G. Christakos, P. Imhoff, J. McBride, J. Pedit, J. Trangenstein, *Adv. Water Res.* **21**, 77 (1998)
49. J. Douglas, F. Pereira, L. Yeh, *Comput. Geosci.* **4**, 1 (2000)
50. B. Riviere, M. Wheeler, *Communi. Numer. Methods Eng.* **18**, 63 (2002)
51. M. Wheeler, M. Peszynska, *Adv. Water Res.* **25**, 1147 (2002)
52. M. Farthing, C. Kees, T. Russell, C. Miller, *Adv. Water Res.* **29**, 657 (2006)

53. N.G. Van Kampen, *Physica* **74**, 215 (1974)
54. G. Sposito, D.A. Barry, Z.J. Kabala, *Advances Porous Media* **1**, 295 (1991)
55. Z.J. Kabala, A. Hunt, *Stochastic Hydrology and Hydraulics* **7**, 255 (1993)
56. S. Kirkpatrick, *Rev. Mod. Phys.* **45**, 574 (1973)
57. A.G. Hunt, *Percolation theory for flow in porous media*, Lecture Notes in Physics (Springer, Berlin, 2005)
58. A. Miller, E. Abrahams, *Phys. Rev.* **120**, 745 (1960)
59. D. Stauffer, A. Aharony, *Introduction to Percolation Theory*, 2nd edn. (Taylor & Francis, London)
60. A.P. Sheppard, M.A. Knackstedt, W.V. Pinczewski, M. Sahimi, *J. Phys. A* **32**, L521 (1999)
61. D. Stauffer, *Phys. Rep.* **54**, 1 (1979)
62. V.N. Ambegaokar, B.I. Halperin, J.S. Langer, *Phys. Rev. B* **4**, 2612 (1971)
63. M. Pollak, *J. Non-Cryst. Solids* **11**, 1 (1972)
64. E.W. Montroll, H. Scher, *J. Stat. Phys.* **9**, 101 (1973)
65. J. Klafter, R. Silbey, *Phys. Rev. Lett.* **44**, 55 (1980)
66. B. Bijeljic, M.J. Blunt, *Water Resour. Res.* **42**, W01202 (2006)
67. H. Scher, E.W. Montroll, *Phys. Rev. B* **12**, 2455 (1975)
68. M. Sahimi, *Rev. Mod. Phys.* **65**, 1393 (1993)
69. M. Sahimi, H. Davis, L. Scriven, *Chem. Eng. Commun.* **23**, 329 (1983)
70. H. Pfannkuch, *Rev. Inst. Fr. Pét.* **2**, L529 (1963)
71. C.H. Seager, G.E. Pike, *Phys. Rev. B* **10**, 1435 (1974)
72. Y. Bernabe, C. Bruderer, *J. Geophys. Res.* **103**, 513 (1998)
73. C.B. Shah, Y.C. Yortsos, *Phys. Fluids* **8**, 280 (1996)
74. G. Dagan, *Rev. Fluid Mech.* **19**, 183 (1987)
75. A.G. Hunt, *Adv. Water Res.* **24**, 279 (2001)
76. M. Rieu, G. Sposito, *Soil Sci. Soc. Am. J.* **55**, 1231 (1991)
77. A.G. Hunt, T.E. Skinner, *Hydrogeol. J.* (2009) doi:10.1007/s10040-009-0499-y
78. E.E. Miller, R.W. Miller, *J. Appl. Phys.* **27**, 324 (1956)
79. P. Moldrup, T. Oleson, T. Komatsu, P. Schjoning, D.E. Rolston, *Soil Sci. Soc. Am. J.* **65**, 613 (2001)
80. A.G. Hunt, R.P. Ewing, *Soil Sci. Soc. Am. J.* **67**, 1701 (2003)
81. A. Hunt, *Solid State Commun.* **80**, 151 (1991)
82. B. Berkowitz, I. Balberg, *Water Resour. Res.* **29**, 775 (1993)
83. B.B. Mandelbrot, *The Fractal Geometry of Nature* (Freeman, 1982)
84. H.J. Herrmann, H.E. Stanley, *J. Phys. A* **21**, L829 (1988)
85. Y. Lee, J.S. Andrade, S.V. Buldyrev, N.V. Dokholoyan, S. Havlin, P.R. King, G. Paul, H.E. Stanley, *Phys. Rev. E* **60**, 3425 (1999)
86. I. Balberg, *Philos. Mag. B* **30**, 991 (1987)
87. A.G. Hunt, *Philos. Mag.* **85**, 3409 (2005)
88. K. Mallory, *Phys. Rev. B* **47**, 7819 (1993)
89. H. Scher, R. Zallen, *J. Chem. Phys.* **53**, 3759 (1970)
90. D. Wilkinson, J. Willemsen, *J. Phys. A* **16**, 3365 (1983)
91. A.M. Shapiro, *Water Resour. Res.* **37**, 507 (2001), doi:10.1029/2000WR900301
92. M.W. Becker, A.M. Shapiro, *Water Resour. Res.* **36**, 1677 (2000)
93. M.W. Becker, A.M. Shapiro, *Water Resour. Res.* **39**, 1024 (2003)
94. Z.-F. Liu, X.-H. Wang, P. Mao, Q.-S. Wu, *Chin. Phys. Lett.* **20**, 1969 (2003)
95. Q. Zhou, H.-H. Liu, F.J. Molz, Y. Zhang, G.S. Bodvarsson, *J. Contam. Hydrol.* **93**, 161 (2007)
96. L. Neretnieks, *J. Geophys. Res.* **85**, 4379 (1980)
97. Q. Zhou, H.H. Liu, G.S. Bodvarsson, C.M. Oldenburg, *J. Contam. Hydrol.* **60**, 1 (2003)
98. P. Maloszewski, A. Zuber, *J. Hydrol.* **79**, 333 (1985)
99. P. Maloszewski, A. Zuber, *Water Resour. Res.* **26**, 1517 (1990)
100. P. Maloszewski, A. Zuber, *Water Resour. Res.* **29**, 2723 (1993)
101. A.F. Moench, *Water Resour. Res.* **31**, 1823 (1995)
102. P. Reimus, G. Pohll, T. Mihevec, J. Chapman, M. Haga, B. Lyles, S. Kosinski, R. Niswonger, P. Sanders, *Water Resour. Res.* **39**, 1356 (2003), doi:10.1029/2002WR001597
103. C.A. Aggelopoulos, C.D. Tsakiroglou, *Water Air Soil Pollut.* **185**, 223 (2007)
104. J.C. Seaman, P.M. Bertsch, M. Wilson, J. Singer, F. Majis, S.A. Aburime, *Vadose Zone J.* **6**, 373 (2007)
105. J. Vanderborght, H. Vereecken, *Vadose Zone J.* **6**, 29 (2007)
106. R. Haggerty, C.F. Harvey, C. Freiherr von Schwerin, L.C. Meigs, *Water Resour. Res.* **40** (2004), doi:10.1029/2002WR001716
107. R. Haggerty, Matrix diffusion: Heavy-tailed residence time distributions and their influence on radionuclide retention, in *Radionuclide Retention in Geologic Media, Workshop Proceedings* (Oskarshamn, Sweden, 2001), *Radioactive Waste Management GEOTRAP Project*, Organisation for Economic Cooperation and Development (2002), pp. 81–90
108. S.P. Neuman, V. Di Federico, *Rev. Geophys.* **41**, 1014 (2003)
109. C. Danquigny, P. Ackerer, J.P. Carlier, *J. Hydrol.* **294**, 196 (2004)
110. S.P.K. Sternberg, J.H. Cushman, R.A. Greenkorn, *Transp. Porous Media* **23**, 135 (1996)
111. D.-J. Kim, J.-S. Kim, S.-T. Yun, S.-H. Lee, *Hydrol. Process.* **16**, 1955 (2002), doi:10.1002/hyp.395
112. H. Chao, H. Rajaram, T. Illangasekare, *Water Resour. Res.* **36**, 2869 (2000)
113. T. Baumann, S. Müller, R. Niessner, *Water Res.* **36**, 1213 (2002)
114. D. Schulze-Makuch, *Ground Water* **43**, 443 (2005)
115. S.P. Neuman, *Ground Water* **44**, 139, and author's reply 140 (2006)
116. M.Y. Corapcioglu, P. Fedirchuk, *J. Contam. Hydrol.* **36**, 209 (1999)
117. W.E. Huang, S.E. Oswald, D.N. Lerner, C.C. Smith, C. Yheng, *Environ. Sci. Technol.* **37**, 1905 (2003)
118. M. Xu, Y. Eckstein, *Ground Water* **33**, 905 (1995)
119. H. Makse, J.S. Andrade, H.E. Stanley, *Phys. Rev. E* **61**, 583 (2000)
120. D. Stauffer, D. Sornette, *Physica A* **252**, 271 (1998)
121. P. Rigord, A. Calvo, J. Hulin, *Phys. Fluids, A Fluid Dyn.* **2**, 681 (1990)
122. G.A. Gist, A.H. Thompson, A.J. Katz, R.L. Higgins, *Phys. Fluids A* **2**, 1533 (1990)
123. J. Koplik, S. Redner, D. Wilkinson, *Phys. Rev. A* **37**, 2619 (1988)
124. V. Gupta, R. Bhattacharya, *Adv. Appl. Probab.* **16**, 18 (1984)

125. V. Gupta, R. Bhattacharya, *Water Resour. Res.* **19**, 945 (1983)
126. B. Bijeljic, M.J. Blunt, *Water Resour. Res.* **42**, W01202 (2006)
127. B. Bijeljic, A. Muggeridge, M. Blunt, *Water Resour. Res.* **40**, W11501 (2004)
128. D. Yu, K. Jackson, T. Harmon, *Chem. Eng. Sci.* **54**, 357 (1999)
129. H. Scher, M.F. Shlesinger, J.T. Bendler, *Phys. Today* **44**, 26 (1991)
130. G. Pfister, C.H. Griffiths, *Phys. Rev. Lett.* **40**, 659 (1978)
131. G. Pfister, *Phys. Rev. Lett.* **35**, 1474 (1974)
132. T. Tiedje, in *Semiconductors and Semimetals*, edited by J. Pankove (Academic, New York, 1984), Vol. 21C, p. 207
133. G. Pfister, *Phys. Rev. Lett.* **36**, 271 (1976)
134. F.C. Bos, T. Guion, D.M. Burland, *Phys. Rev. B* **39**, 12633 (1989)
135. G. Pfister, H. Scher, *Phys. Rev. B* **15**, 2062 (1977)
136. R. Metzler, J. Klafter, *Phys. Rep.* **339**, 1 (2000)
137. M. Marseguerra, A. Zoia, *Math. Comput. Simul.* **77**, 345 (2008)
138. B. Berkowitz, A. Cortis, M. Dentz, H. Scher, *Rev. Geophys.* **44** (2006), doi:10.1029/2005RG000178
139. S. Redner, S. Datta, *Phys. Rev. Lett.* **84**, 6018 (2000)
140. A.D. Araujo, J.S. Andrade, H.J. Herrmann, *Phys. Rev. Lett.* **97**, 138001 (2006)
141. E.A. Sudicky, *Water Resour. Res.* **22**, 725 (1986)
142. E.A. Sudicky, J.A. Cherry, E.O. Frind, *J. Hydrol.* **63**, 81 (1983)
143. D.M. Mackay, D.L. Freyberg, P.B. Roberts, J.A. Cherry, *Water Resour. Res.* **22**, 2017 (1986)
144. P.V. Roberts, M.N. Goltz, D.M. Mackay, *Water Resour. Res.* **22**, 2047 (1986)
145. C. Rivard, F. Delay, *Hydrogeol. J.* **12**, 613 (2004)
146. M. Javaux, M. Vanclooster, *Soil Sci. Soc. Am. J.* **67**, 1334 (2003)
147. C.W. Rovey, W.L. Niemann, *Ground Water* **43**, 52 (2005)
148. R. Ramanathan, R.W. Ritzi, C.C. Huang, *Water Resour. Res.* **44**, W04503 (2008), doi:10.1029/2007WR006282
149. R. Ramanathan, R.W. Ritzi, R.M. Allen-King, *Water Resour. Res.* **46**, W01510 (2009)